Ecological Modelling 151 (2002) 75–108

ECOLOGICAL MODELLING

www.elsevier.com/locate/ecolmodel

A simulation model linking crop growth and soil biogeochemistry for sustainable agriculture

Yu Zhang [a,b,*], Changsheng Li [c], Xiuji Zhou [b], Berrien Moore III [c]

[a] *Department of Geophysics, Peking University, Beijing 100871, People's Republic of China*

[b] *Chinese Academy of Meteorological Sciences, Beijing 100081, People's Republic of China*

[c] *Complex Systems Research Center, Institute for the Study of Earth, Oceans and Space, University of New Hampshire, Durham, NH 03824, USA*

Received 23 January 2001; received in revised form 19 September 2001; accepted 18 October 2001

Abstract

Predicting impacts of climate change or alternative management on both food production and environment safety in agroecosystems is drawing great attention in the scientific community. Most of the existing agroecosystem models emphasize either crop growth or soil processes. This paper reports the latest development of an agroecosystem model (Crop-DNDC) by integrating detailed crop growth algorithms with an existing soil biogeochemical model, DNDC (Li et al., J. Geophys. Res. (1992) 9759). In the Crop-DNDC model, crop growth is simulated not only by tracking crop physiological processes (phenology, leaf area index, photosynthesis, respiration, assimilate allocation, rooting processes and nitrogen uptake), but also by calculating water stress and nitrogen stress, which were closely related to soil biogeochemical processes and hydraulic dynamics. Crop-DNDC also quantifies crop residue incorporated in the soil at the end of each growing season. Thus the model has tightly coupled crop growth algorithms with soil biogeochemical components, and simulates carbon, nitrogen and water cycles in agroecosystems with a relatively complete scope. The model was validated against field measurements, including soil moisture, leaf area index, crop biomass and nitrogen content, and the modeled results were in agreement with observations on soil carbon dynamics and trace gas emissions as well. Sensitivity tests demonstrated that the modeled results in crop yield, soil carbon dynamics and trace gas emissions were sensitive to climate conditions, atmospheric CO_2 concentration and various farming practices. There are potentials of applying the model for simultaneously predicting effects of changes in climate or management on crop yield, soil carbon sequestration and trace gas emissions.

Keywords: Model; Crop; Soil biogeochemistry; Sustainable agriculture

1. Introduction

Agriculture is an essential industry supporting the increasing population on our planet. Modern technology has greatly promoted agricultural pro-

* Corresponding author. Environmental Monitoring Section, Canada Center for Remote Sensing, 588 Booth Street, Ottawa, Ontario, Canada K1A 0Y7. Tel.: +1-613-947-1367; fax: +1-613-947-1383.

E-mail address: yu.zhang@ccrs.nrcan.gc.ca (Y. Zhang).

PII: S0304-3800(01)00527-0

ductivity by means of genetic improvement, irrigation, fertilization and pesticide applications. But food security is still a primary concern today, and it will be so in the future because of the contradiction between the increases in human population and rising standards of living, and the limitation of natural resources. Meanwhile, agriculture is also an important aspect of human activity that profoundly influences global environment, such as atmospheric chemistry, water quality and quantity, and nutrient cycles. For example, nitrogen fertilizer production and application and crop biological fixation have doubled the transfer of nitrogen from the atmosphere to biologically available pools (Vitousek et al., 1997), and that would substantially increase nitrogenous gas emissions to the atmosphere. It is estimated that 80% of nitric oxide (NO), nearly 70% of ammonia (NH_3) and more than 40% of nitrous oxide (N_2O) emitted globally are human-activity induced (Vitousek et al., 1997), and agriculture accounts for 92% of total anthropogenic emissions of N_2O (Duxbury et al., 1993). Agricultural activity can increase carbon dioxide (CO_2) emissions to the atmosphere by increasing soil decomposition rate and burning plant biomass. Paddy rice field is also an important source of atmospheric methane (CH_4). It is estimated that agriculture accounts for 26 and 65% of the total anthropogenic emissions of CO_2 and CH_4, respectively (Duxbury et al., 1993). Balancing food production and environmental protection, and predicting the impacts of climate change or alternative management on both food production and environment safety in agroecosystems are drawing great attention in the scientific community.

Agroecosystems include complex components and processes of soil, crops, the atmosphere and farming practices. Dynamic modeling is an effective approach to characterize the whole system by integrating various processes, and a model can be used as a tool for mechanism understanding, estimating, predicting, and policy making. There have been lots of modeling studies around agroecosystems in the fields of agronomy, climatology, and environmental studies, although their purposes, approaches and scales are quite different. Agronomists pay more attention to crop growth and yield formation. Their models are usually called crop growth models, such as DSSAT (Tsuji et al., 1994), RCSODS (Gao et al., 1992) and modeling studies by de Wit (1978) and his colleagues in Wageningen (e.g. Penning de Vries et al., 1989). The purposes of these models focus on high crop production and efficient management, especially for water and fertilizer management. Usually crop growth, development and soil water dynamics are simulated in detail, but soil biogeochemistry is not considered or simply simulated in terms of nutrient effects on crops in the models. Environmental studies focus on element and material cycles. Their models are usually termed as biogeochemical models, such as RothC (Jenkinson, 1990) for organic carbon turnover, CENTURY (Parton et al., 1988) for carbon, nitrogen, sulphur and phosphorus cycles, DNDC (Li et al., 1992a,b) and CASA (Potter et al., 1996) for N_2O emissions, and MEM (Cao et al., 1995) for CH_4 emissions. These models pay more attention to soil processes, such as decomposition, nitrification and denitrification, etc. Climatologists are interested in the boundary effects of soil and vegetation on the movement of the atmosphere. Their soil–crop related models are usually called land-surface parameterization, such as SiB (Sellers et al., 1986) and BATs (Dickinson et al., 1986). These models pay more attention to physical processes, such as radiation, water, heat and momentum fluxes. Therefore gaps exist among the modeling efforts of agronomists, environmentalists and climatologists due to their different focuses. This study reports the development of the DNDC model (Li et al., 1992a) by integrating crop growth processes with soil biogeochemistry.

The DNDC model (DeNitrification and DeComposition) was originally designed to simulate soil carbon and nitrogen dynamics and trace gas emissions (Li et al., 1992a). Crop growth was estimated using a generalized crop growth curve (Li et al., 1994a,b). Therefore the model did not consider the effects of climate on crop growth and its interactions with soil biogeochemical processes. There are some crop models (such as DSSAT, Tsuji et al., 1994) simulating crop growth with impacts of climate and soil conditions, although simply linking this kind of detailed crop models to

DNDC may not be very easy or efficient. In our study, several key crop growth algorithms were developed and integrated with the soil processes in DNDC to improve its ability in predicting crop growth with a reasonable coding innovation. With the enhanced crop growth submodel, the newly developed Crop-DNDC model has come out with a relative complete feedback between crop growth and soil biogeochemical processes.

2. Model description

2.1. The overall structure

Fig. 1 shows the overall structure of the model. The major considerations for the model development include: (1) the dynamics of crop growth and its responses to climatic conditions and farming practices; (2) interactions of crop growth with soil biogeochemical processes, and (3) the overall behavior of the model in simulating crop yield and trace gas emissions responding to climate conditions and management practices. The model consists of three submodels. Climatic submodel calculates water dynamics and soil temperature profile. Crop submodel simulates crop phenological development, leaf area index (LAI), photosynthesis, respiration, assimilate allocation, rooting processes and nitrogen uptake. Soil biogeochemistry submodel predicts decomposition, nitrification, denitrification and trace gas emissions. Crop growth interacts with soil climatic and biogeochemical submodels in terms of water and nitrogen uptake, water and nitrogen stress on crop growth, and the amount and quality of crop residue incorporated in the soil at the end of the growing season. Thus the model tightly couples crop growth with soil biogeochemical and climatic components, and simulates C, N and water cycles in agroecosystems with a relatively complete scope. The input data include climate drivers, soil features, crop parameters and farming practices. The output includes soil carbon and nitrogen pools and fluxes, crop production, nitrate leaching and trace gas emissions. The primary time step of the simulation is 1 day. Spatially, state variables are expressed as mass per unit area (such as kg/ha) or relative content (fraction), they may represent a site, a field or an area where its size depends on the degree of homogeneity of the area and the representativeness of the input data. Soil profile is divided into numerous layers and simulation is conducted layer by layer.

2.2. Climate submodel

2.2.1. Day length, solar radiation and temperature

Day length is estimated based on latitude and Julian date (Spitters et al., 1986. See Appendix A for the equations). Photosynthetically active radiation at a certain time of the day is estimated based on daily solar radiation and solar elevation (Spitters et al., 1986; Kropff and van Laar, 1993). Users can directly input daily solar radiation, or the model can derive solar radiation from daily sunshine duration or from the range of daily temperature extremes based on empirical estimations of daily transmission coefficient of solar radiation (Briston and Cambell, 1984).

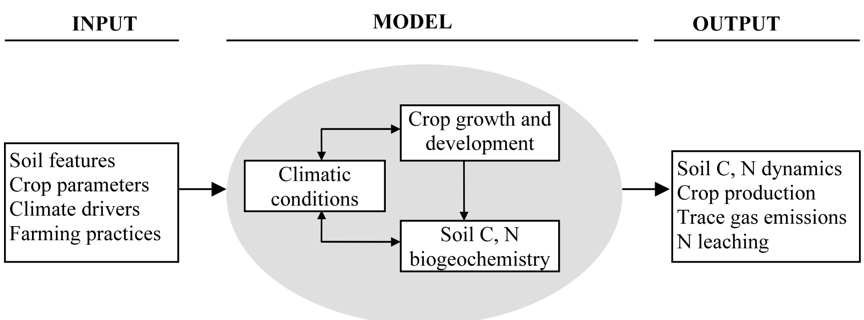

Fig. 1. The overall structure of the Crop-DNDC model.

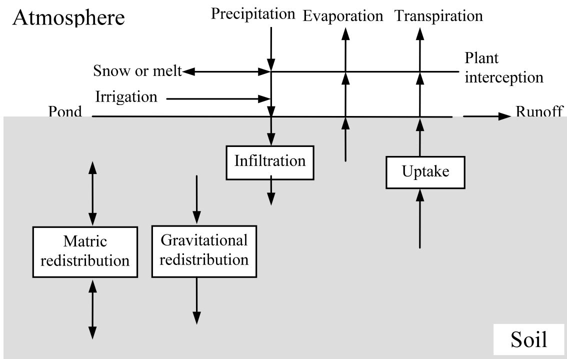

Fig. 2. The scheme of the water submodel.

Canopy and soil temperatures are estimated based on daily air maximum and minimum temperatures. We assume that canopy temperature equals air temperature observed in thermometer screens about 1.5 m above the surface except where snow cover exists. The effect of snow cover on canopy temperature is estimated based on Ritchie et al. (1988). Daily and daytime mean canopy temperatures are estimated based on daily maximum and minimum canopy temperatures. The hourly canopy temperature is simulated using a sine function for daytime and an exponential function for nighttime (William and Logan, 1981). Soil temperature is simulated as a cosine function of Julian date with an exponentially decreased amplitude with depth, and considering the influence of the current surface temperature and soil moisture (Williams, 1995).

2.2.2. Soil moisture

The scheme of soil water submodel is based on Ritchie et al. (1988) (Fig. 2). Water movement is simulated considering the processes of surface runoff, infiltration, gravitational and matric redistribution, evaporation and transpiration. Water available for infiltration includes rainfall, irrigation, snow melt and pond existing on the surface. Precipitation is considered as snowfall when daily mean air temperature is below zero, and precipitation may be intercepted by crop canopy as well. The water above the surface may be lost as surface runoff and evapotranspiration. The model estimates daily surface runoff based on the SCS curve procedure (US Department of Agriculture, Soil Conservation Service, 1972; Williams, 1995). Water will infiltrate into soil profile layer by layer until all the water on the surface is depleted or the infiltration is limited by time (over 24 h) or by a frozen layer. In the latter two cases, the remaining water will stay on the surface as pond. Gravitational redistribution here means the downward water flow when soil moisture is higher than field capacity. We assume a fraction (the model uses 0.5 as the default value based on Ritchie et al., 1988) of water above field capacity will be drained everyday. Matric redistribution here means water downward or upward movement because of the moisture difference (more exactly, the potential difference) of adjacent soil layers. It is simulated based on Ritchie et al. (1988). Potential evapotranspiration is estimated based on the Priestly–Taylor approach (1972) using solar radiation and temperature (Ritchie et al., 1988). Potential evapotranspiration is separated into potential evaporation and potential transpiration based on LAI (Ritchie, 1972). Based on Dhakhwa et al. (1997), we assume potential transpiration decreases 30% when atmospheric CO_2 concentration doubles. Actual plant transpiration is jointly determined by potential transpiration (demand) and crop uptake capacity (provision), which depends on soil moisture and root conditions (amount and distribution). Flooding (for paddy rice) is mainly controlled by farming practices. During flooding period, all the soil profile is saturated and water redistribution processes are not considered.

2.3. Crop submodel

Fig. 3 shows the structure of the crop submodel. The major state variables include phenological development, LAI, biomass and nitrogen content of crop organs. Crop assimilates atmospheric carbon through photosynthesis, and carbon assimilation produces nitrogen demand. The actual nitrogen uptake also depends on the availability of mineral nitrogen in soil. Phenological stages and stress factors (water and nitrogen) influence carbon allocation and nitrogen demand. The major processes of the crop submodel includes phenological development, LAI, photosyn-

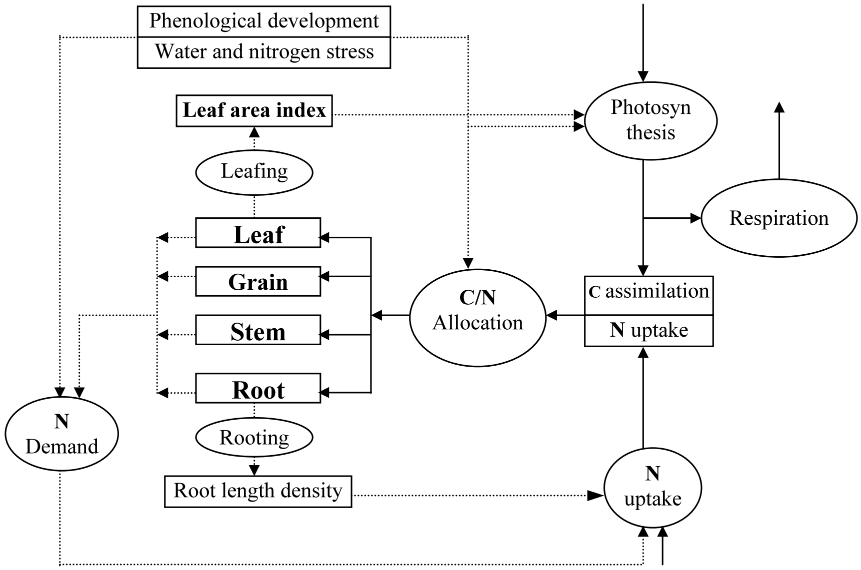

Fig. 3. The scheme of the crop submodel (rectangles are for state variables, and circles/ellipses are for processes; solid lines and dash lines are for matter flow and information flow, respectively).

thesis and respiration, assimilate allocation, rooting processes, water and nitrogen uptake. In this study we try to use common approaches and reduce the differences in crop features to parameters. Currently the crop submodel includes wheat, rice and corn.

2.3.1. Phenological development

A life cycle of crops is divided into nine phenological development stages based on CERES models (Ritchie, 1991; Ritchie et al., 1988, 1987). Active crop growth stages are from emergence to maturity (Table 1). Phenological development rate is simulated based on thermal time (Ritchie, 1991; Jones and Kiniry, 1986)

$$\mathrm{DR} = \mathrm{Dtt}/P_i \tag{1}$$

where DR is daily development rate, and P_i is the total thermal time needed for completing a given stage i. Dtt is daily thermal time, calculated based on temperature

$$\mathrm{Dtt} = \frac{1}{24}\sum_{i=1}^{2} \min[T_{\mathrm{Dm}} - T_{\mathrm{Db}}, \max(0, T_{\mathrm{c}}(t) - T_{\mathrm{Db}})] \tag{2}$$

where $T_{\mathrm{c}}(t)$ is hourly canopy temperature at time t, T_{Dm} and T_{Db} are maximum and basal temperatures for development, respectively. The basal temperature is 1, 10 and 8 °C for wheat, rice and corn, respectively, and the maximum temperature is 34 °C for all these three crops (Penning de Vries et al., 1989). The thermal time needed from

Table 1
Phenological development stages and their corresponding numerical scales (Ritchie et al., 1988, 1987; Jones and Kiniry, 1986)

Stage no.	*xs* scale	*zs* scale	Event description
7	–	–	Sowing
8	–	–	Germination
9	0.0	0.0	Emergence
1	1.0	1.5	Beginning floral initiation
2	2.0	4.5	End floral initiation
3	3.0	6.0	Flowering
4			Beginning grain filling
5	4.0	10.0	Maturity
6	–	–	Harvest

Note: Stage number is for a period from last event to current event. *xs* and *zs* are continuous scales. Their daily values are interpolated based on thermal or photothermal time.

sowing to emergence (P_9) is estimated based on sowing depth (SD, in cm)

$$P_9 = 40 + 10\text{SD} \quad (3)$$

For other stages, the amounts of thermal time needed are input genetic parameters or estimated based on thermal time of the former stages. For wheat, the development from emergence to terminal spikelet initialization (stage 1) is simulated considering both vernalization and photoperiodism effects (Ritchie, 1991). The thermal time needed for the following three stages are estimated based on phyllochron parameter, which is defined as the interval of thermal time between leaf tip appearance (Ritchie, 1991). The thermal time needed for grain filling (stage 5) is an input parameter. For rice and corn, the thermal time needed from emergence to beginning floral initiation (stage 1) and in grain filling stage (stage 5) are determined by user as input genetic parameters. Floral initiation (stage 2) is the stage of photoperiodism for corn and rice. It is estimated based on day length using two input parameters: sensitivity to day length and critical day length (the development rate will be limited when day length is longer than the critical day length). The thermal time accumulated in stage 2 is used to estimate the thermal time needed for stage 3 (from the end of floral initiation to flowering) based on Ritchie (1991) and Kiniry (1991). The thermal time needed from flowering to the beginning of grain filling is fixed as 170 °C d (Ritchie, 1991; Kiniry, 1991; Ritchie et al., 1987).

2.3.2. Leaf area index (LAI)

LAI variation is simulated as the difference between leaf area growth (associated with assimilate allocation) and leaf senescence (associated with phenological development and stress factors).

$$\Delta\text{LAI} = \text{GroL} - \text{SenL} \quad (4)$$

where ΔLAI is the daily variation of LAI, GroL and SenL is the daily leaf area growth and senescence, respectively. The simulation for wheat is based on the relationship between leaf and tiller numbers of one crop stand (Ritchie et al., 1988). For rice and corn, early LAI growth is simulated using an exponential function of thermal time (Kropff and van Laar, 1993) and leaf number (Jones and Kiniry, 1986), respectively. After that, LAI growth is simulated according to the assimilates allocation. Leaf senescence is estimated based on phenological stages and the effects of water and nitrogen stress factors (Ritchie et al., 1988; Jones and Kiniry, 1986).

2.3.3. Photosynthesis, respiration and assimilate allocation

Gross photosynthesis is simulated based on Spitters (1986) and Spitters et al. (1986) considering direct and diffuse light separately. The integration of photosynthesis rate with time and canopy profile is conducted using Goudriaan's (1986) three-point Gaussian integration method. The response of photosynthesis to light is expressed as an exponential function with two parameters (Penning de Vries et al., 1989). The effects of temperature on photosynthesis are simulated as influencing photosynthesis rate at light saturation and initial light use efficiency (Penning de Vries et al., 1989). The effect of atmospheric CO_2 concentration on photosynthesis rate is considered based on Goudriaan et al. (1984). Photosynthesis is also influenced by water and nitrogen stress factors.

Crop respiration is simulated considering growth and maintenance respiration separately (McCree, 1979). Maintenance respiration is calculated based on temperature and biomass of crop organs. Growth respiration is estimated based on the amount of assimilate available for growth. Maintenance respiration coefficients and growth efficiency coefficients are from Penning de Vries et al. (1989).

The difference between gross photosynthesis and respiration is the amount of assimilate available for allocation among crop organs. Assimilate allocation is simulated based on phenological stages (Penning de Vries et al., 1989; Ritchie et al., 1988). At first the model estimates the partitioning of assimilate between shoot (leaf, stem and grain) and root, then the model calculates the partitioning among leaf, stem and grain (Table 2). During grain filling period, the potential grain growth is simulated based on Ritchie et al. (1988) for wheat

Table 2
Assimilate partitioning among plant organs

Fraction of assimilate partitioned to shoot (F)			
Stage	Wheat	Rice	Corn
1	GroL/Sla/Asm	0.5+0.2xs	(0.5+0.15xs)[0.5+0.5 min(ws,ns)]
2	0.7+0.1 min(ws,ns)	0.7+0.2xs	[0.65+0.1(xs−1)][0.8+0.2 min(ws,ns)
3	0.75+0.1 min(ws,ns)	0.9	[0.75+0.1(xs−2)][0.9+0.1 min(ws,ns)]
4	0.8+0.1 min(ws,ns)	0.9+0.1(xs−3)	[0.85+0.15(xs−3)][0.9+0.1 min(ws,ns)]
5	0.65+0.3 BM_{Stem0}/BM_{Stem}	0.9+0.1(xs−3)	1

Fraction of assimilate partitioned to leaf, stem and grain				
Crop	Stage	Leaf	Stem	Grain
Wheat	1	F	0	0
	2	(1−0.12Tdtt/Phr)F−0.1	0.15+0.12Tdtt/Phr−F	0
	3, 4	0	F	0
Rice	1	[0.5+0.15(1+xs)]F	[0.5−0.5(1−xs)]F	0
	2	0.5F	0.5F	0
	3	0.5(3−xs)F	[1−0.5(3−xs)]F	0
	4	0	(4−xs)F	(xs−3)F
	5	0	0	1
Corn	1	0.6F	0.4F	0
Corn	2	[0.6+0.25(xs−1)]F	[0.4−0.25(xs−1)]F	0
	3	[0.35−0.25(xs−2)]F	0.65F	0.25(xs−2)F
	4	0.1(4−xs)F	0.65(4−xs)F	0.25(4−xs)F

Note: Asm is the amount of daily assimilate, GroL is increase rate of LAI, Sla is specific leaf area. BM_{Stem0} is stem biomass at flowering. BM_{Stem} is current stem biomass. ws and ns are water and nitrogen stress factors ranging from zero to one (one is for no constraint, zero is for maximum constraint). Tdtt is the accumulated thermal time in the current stage. Phr is phyllochron. xs is a development scale. In stage 5, wheat and corn partition assimilate according to the requirement of grain growth.

and based on Jones and Kiniry (1986) for corn. If the assimilate is not enough for grain growth requirement, the deficiency will be translocated from stem, otherwise the stem will get the remains. For rice, the contribution of pre-heading storage to grain yield is about 20–40% (Yoshida, 1972; Gao et al., 1992), that is about 1% per day for a typical grain filling stage. We simply assume that 1% of the stem biomass will be translocated to grain every day during grain filling period.

2.3.4. Rooting process, and water and nitrogen uptake

Rooting processes include the increase of root front depth, the distribution of root length density and biomass in soil profile. In the model, the deepening rate of root front is proportional to thermal time before flowering, and root front depth is limited to a maximum depth (1 m). Daily variation of root length density in a layer depends on new root growth and root senescence. The assimilate partitioned to root determines new root growth. Daily root senescence is assumed as 1–2% of the total root biomass depending on stress factors. Root biomass distribution in soil profile is estimated based on root length distribution, which follows an exponential pattern in soil profile (Jones et al., 1991), but it is subjected to the influence of constraint factors. In the Crop-DNDC model, constraint factors (ranging from 0 to 1) for each layer include a static factor and four dynamic factors. The static factor of each layer is a direct input parameter (it varies with soil depth) for the effects of toxicity, coarse fragments, plough pan layer, deficiency of nutrients other than nitrogen, etc. Dynamic constraint factors include the effects of soil strength, aeration, temperature and nitrogen. Soil strength factor is estimated based on soil bulk density, soil texture and water content (Jones et al., 1991). Aeration factor depends on soil moisture and sensitivity of plant to water saturation (related with plant aerenchyma). Nitrogen factor is simulated based on Ritchie et al. (1988).

Crop water uptake depends on potential transpiration demand determined by LAI and climate conditions and uptake capacity determined by soil moisture, root length and its distribution in soil. We assume that roots are uniform line sinks with a specific uptake capacity, and soil moisture influences the actual uptake capacity. Water stress factor is estimated based on the ratio of actual water uptake and potential transpiration demand (Ritchie et al., 1988).

Crop nitrogen uptake depends on crop demand and uptake capacity. Crop demand is simulated based on the assumption that at any time plant has a critical nitrogen concentration below which plant growth will be reduced (Godwin and Jones, 1991). This principle is also used for estimating nitrogen stress. Nitrogen demand includes deficiency demand (restoring to the critical concentration) and new growth demand associated with carbon assimilation and allocation. Nitrogen uptake capacity depends on mineral nitrogen concentration in root zone and soil moisture, which are simulated by soil biogeochemical and hydrological components. Nitrogen demand and uptake capacity are simulated based on Godwin and Jones (1991). Crop nitrogen pools are divided into shoot (leaf and stem), grain and root. Nitrogen will be partitioned to shoot and root according to their demand (we assume that shoot and root have the same relative nitrogen concentration compared to their critical concentrations).

2.4. Submodel of soil carbon and nitrogen biogeochemistry

Soil carbon and nitrogen biogeochemical processes are simulated based on the DNDC model (Li et al., 1992a,b) (Fig. 4). Soil organic carbon is divided into three active pools and one passive pool, and each active pool is further divided into two or three subpools. The decomposition of each pool is simulated with first-order kinetics. Actual decomposition rate also depends on environmental factors, including temperature, moisture, nitrogen availability, soil texture (clay adsorption) and farming practices (soil disturbance). Crop litter or manure will be partitioned into the residual pools according to its C/N ratio. During decomposition of residual pools, the carbon decomposed will be partitioned to microbial pools and CO_2. Under anaerobic conditions, CO_2 and some small molecular carbon substrates may be converted to CH_4. Soil redox potential is estimated based on flooding conditions. CH_4 emission is the difference between production and oxidation. The production and oxidation rates are simulated based on Cao et al. (1995).

During decomposition, soil organic nitrogen will decompose and transfer to ammonium (NH_4^+). NH_4^+ can be oxidized to nitrate (NO_3^-) under aerobic conditions (nitrification), or can be absorbed by clay particles, or transformed into ammonia (NH_3) which can be released to the atmosphere. Both NH_4^+ and NO_3^- are subject to plant uptake and microbe assimilation. NO_3^- movement in soil solution is simulated as mass flow with water flux and diffusion driven by concentration gradient (Biggar and Nielsen, 1976). Under anaerobic conditions, nitrate can be reduced to NO_2^-, NO, N_2O and N_2 in sequence. The model tracks dynamics of microorganisms, substrate availability and effects of environmental conditions (Li et al., 1992a). The fraction of nitrogen trace gases emitted to the atmosphere is estimated based on soil moisture, temperature, and denitrification kinetics.

3. Model operation

We programmed Crop-DNDC using Turbo C + +, and developed an integrated system for data input/modification, simulation, result analysis and simulation option settings. The code includes a main module, a common procedure module, and five classes for initial data input, simulation, data input during simulation, graphic display and results analysis. The input data include climate, geographic and soil features (soil texture and soil organic carbon content), farming practices and crop genetic parameters. Most of the input items are the same as DNDC model (Li et al., 1992a). Additional input items include crop genetic parameters, atmospheric CO_2 concentration, SCS curve number for surface runoff (US Department of Agriculture, SCS, 1972), average water table depth, daily minimum and maximum temperature (instead of daily mean temperature in DNDC) and solar radiation (it can be estimated from sunshine duration or daily temperature extremes). Crop genetic parameters for phenological development are usually calibrated based on observed development stages. Other genetic parameters (such as photosynthesis rate at light saturation, light extinction coefficient and phyllochron) are relatively stable and can use the model default values. Farming practices include sowing (date, depth, density and crop variety), transplanting of rice (date, depth and plant density), harvest (date and straw management), irrigation (date and amount), flooding (beginning and end dates), fertilization (date, depth, amount

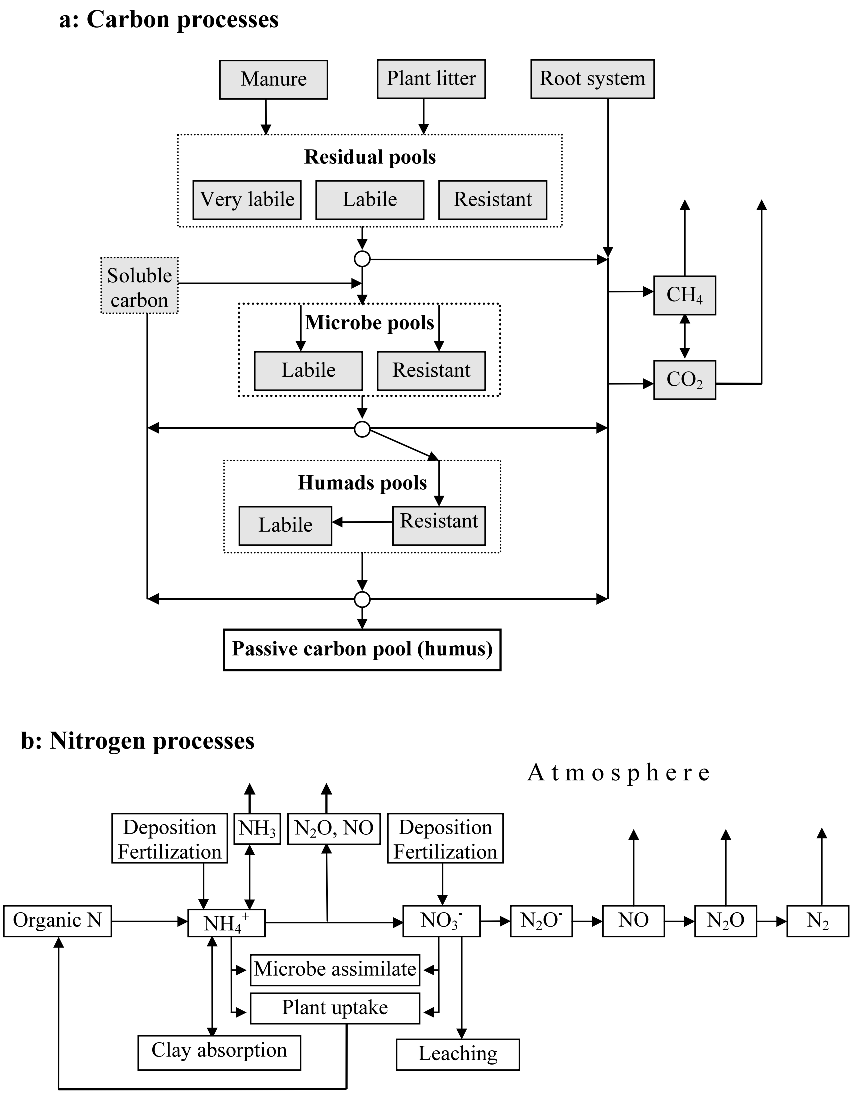

Fig. 4. (a) Soil carbon and (b) nitrogen pools and their transformation processes considered in the Crop-DNDC model (based on Li et al., 1992a).

Table 3
The experiments and model parameters

Experiment case	Case 1	Case 2	Case 3	Case 4
Experiment site	Shandong, China	Jiansu, China	Hunan, China	Iowa, USA
Latitude	36.15°N	32.50°N	28.22°N	41.51°N
Crop	Winter wheat	Winter wheat	Rice	Corn
Major measurements	Soil moisture, LAI, biomass	Soil moisture, LAI, biomass	LAI, biomass	LAI, biomass, plant nitrogen
Bulk density (g/cm^3)	1.38	1.29	1.40	1.30
Clay (fraction)	0.34	0.56	0.26	0.22
Silt (fraction)	0.30	0.35	0.30	0.30
Average water table (m)	8	1.5	Flooding	3
Initial soil organic C (%)	2.0	2.0	3.5	4.1
Water stress on crop	Yes	Yes	No	Yes
Nitrogen stress on crop	No	No	No	Yes
A_{max0} (kg CO_2/ha/hr)[a]	45	45	47	60
K[a,b]	0.6	0.6	0.41^{BH}, 0.68^{AH}	0.65
P_1 (°C d except for wheat)[a,b]	4.5	0.1	500^{C}, 800^{V}, 470^{Z}, 940^{G}	370
P_5 (°C d)[a,b]	500	580	350^{C}, 350^{V}, 250^{Z}, 570^{G}	500
DL_0 (h)[a,b]	20[c]	20[c]	12^{C}, 12.5^{V}, 11.0^{Z}, 13.0^{G}	12.0
f_{DL}[a,b]	1.0	2.5	0^{C}, 10^{V}, 0^{Z}, 30^{G}	0

^{BH} and ^{AH} are for light extinction coefficients of rice before and after heading, respectively (Gao et al., 1992). $^{C, V, Z, G}$ are for cultivars of C-48, V-77, 89Z-229 and GE-1, respectively.
[a] Penning de Vries et al. (1989).
[b] Determined based on comparing with measured phenological stages.
[c] Ritchie et al. (1988).

of nitrate, ammonium, ammonia and urea), manuring (date, depth, amount and C/N ratio) and tilling (date and depth). The system traces the conservation of water, plant biomass, soil organic carbon and inorganic nitrogen, and can graphically display the temporal and spatial distributions of major variables.

4. Validation analysis

4.1. Experiments and data

We selected four crop experiments to validate Crop-DNDC, especially for the newly developed parts of the model, including soil moisture, LAI, crop carbon and nitrogen dynamics of wheat, corn and rice. We also simulated three cases for long-term soil carbon dynamics, N_2O and methane emissions, to ensure that the upgraded model still keeps the capability of DNDC in simulating soil biogeochemical processes. Because soil biogeochemistry and trace gas emissions have been validated extensively (Li et al., 1992b, 1994a,b, 1996, 1997; Li, 2000), this paper focus on the validation of the newly developed parts based on four crop experiments (Table 3).

4.1.1. Case 1. Water experiments in Shandong, China

The Project of North China Plain Crop Water Stress and Drought, 1992 conducted intensive water experiments at Taian Agrometeorological Experimental Station in Shandong Province, China, from 1983 to 1985. The experiments included three winter wheat growing seasons (planted in the early October and harvested in the mid of June next year) and 29 water treatments (nine in 1983–1984, ten in 1984–1985 and 1985–1986 growing seasons each). The water input to the field was controlled by measured irrigation and movable rain-shelters (to avoid undesired water input from precipitation). Soil moisture was measured using neutron probes for about every 10 days during wheat growing season. The layer depth was 5 cm for the two top layers but 10 cm for the deeper layers. Crop biomass (above ground) and LAI were measured for about every 10 days after greening. LAI was measured using a leaf area meter (LI-3100, LICOR, Lincoln, Nebraska). Crop samples were weighed after drying to a stable weight in oven. The soil is deep alluvial loam, and crop cultivar is Lumai No.1. The experiments were designed to study the relationship between crop and water stress, enough nitrogen was provided so we did not consider nitrogen stress on crop growth during simulation.

4.1.2. Case 2. Winter wheat experiments in Jiangsu, China

The experiments were conducted at Zhenjiang Agrometeorological Experimental Station in Jiangsu Province from 1983 to 1985. Winter wheat was planted on different dates (October 18, October 24, November 7 in 1983 and October 20, October 31, November 10 and November 20 in 1984). Soil moisture was measured gravimetrically by taking soil samples (5 cm for the two top layers and 10 cm for other layers). The depth of measurements was 0–40 cm before heading and 50 cm after heading. Crop biomass was measured by harvesting plants randomly from fields, and LAI was estimated from leaf biomass using specific leaf area, which is determined from some sample leaves. The soil is clay loam and water table is about 1–2 m below the surface.

Table 4
Experiments in Hunan, China from 1993 to 1994

Year	Cultivar	Sowing date	Transplanting date
1993	C-48	April 2	May 3
		April 13	May 9
	V-77	June 15	July 26
		June 22	July 23
		July 2	July 28
1994	89Z-229	March 24	May 1
		April 1	May 8
		April 7	May 16
	GE-1	June 10	July 14
		June 14	July 14
		June 22	July 20

4.1.3. Case 3. Rice experiments in Hunan, China

The experiments were conducted at Changde Agrometeorological Experimental Station in Hunan Province, China, from 1993 to 1994. There were 11 plantings and four cultivars in the experiments. Table 4 shows the sowing and transplanting dates of each cultivar. LAI and biomass of each organ were measured by randomly harvesting 10–15 plants for about every 5 days after transplanting. The fields were flooded, and soil fertility was kept high. Rice growth is simulated without considering water and nitrogen stress. Daily weather data were from the local meteorological observatory.

4.1.4. Case 4. Corn experiment in Iowa, USA

The field experiments were conducted at Mascutine, Iowa, USA in 1997 and 1998. The experiment was intended to link field measurements, remotely sensed information and a simulation model, therefore the observations were conducted at a typical corn field without any special treatment. LAI was measured for about every week using a LAI2000 Leaf Canopy Analyzer (LICOR, Lincoln, Nebraska). At the same time, 3–20 plants were sampled randomly for biomass and crop nitrogen measurement. Plant samples were dried and weighed for each organ (root, grains and straw), and the nitrogen concentration was measured using the ground samples of each organ. The daily maximum and minimum temperature data are from Iowa City observatory (http://www.nndc.noaa/cgi-bin/nndc/buyOL-002.cgi), and daily solar radiation data are from re-analysis data provided by the NOAA-CIRES Climate Diagnostic Center, Colorado (http://www.cdc.noaa.gov/).

Table 5
Correlation coefficient between simulated and measured values for the experiments in Shandong, China (three winter wheat growing seasons from 1983 to 1986)

Year		1983–1984	1984–1985	1985–1986	Average
No. of moisture measurements		67	104	105	
No. of crop measurements		60	80	80	
Soil moisture	0–10 cm	0.3014	0.4185	0.5965	0.4388
	10–20 cm	0.5832	0.4821	0.5273	0.5309
	20–30 cm	0.6870	0.4919	0.6362	0.605
	30–40 cm	0.6767	0.6288	0.6836	0.663
	40–50 cm	0.6509	0.7577	0.7429	0.7172
	0–50 cm	0.7327	0.6064	0.7164	0.6852
LAI		0.9221	0.8929	0.8597	0.8916
Aboveground biomass		0.9404	0.9334	0.9356	0.9365

4.2. Initial conditions and model parameters

Initial soil temperature is estimated based on annual average temperature and amplitude, and the day of year on which simulation begins. Soil moisture is set to field capacity. We run the model one or more months before sowing (usually from the first day of the year) so that soil moisture and temperature can get an equilibrium with the actual climate conditions before crop growth. Latitude, soil texture and soil organic carbon content were determined based on site measurements (Table 3). Soil hydrological parameters (wilting point, field capacity and porosity) were estimated based on soil texture (Saxton et al., 1986). SCS curve number for surface runoff (US Department of Agriculture, SCS, 1972) used a value of 84 based on field slope and texture (Ritchie et al., 1988). We simulated crop growth according to the farming practices of the experiments (sowing, transplanting, irrigation, flooding, and fertilization). Crop maximum photosynthesis rates and light extinction coefficients are the model default values which are from Penning de Vries et al. (1989). Crop phenological development parameters (the thermal time needed from emergence to beginning floral initiation, and in grain filling stages, critical day length and the sensitivity to photoperiodism) were calibrated based on measured phenological stages (mainly heading, flowering and maturity). Once the parameter values are determined, they are used for all the plantings of this cultivar.

4.3. Comparison of simulated results with measurements

4.3.1. Soil moisture

In the Shandong experiments (Case 1), soil moisture are usually high in the fall and early spring, and then decline until the rain season begins. Crop-DNDC captured this variation pattern well. Comparing to measurements, the simulation results were better for the natural conditions than for the water treatment conditions, that may be because there is a higher soil heterogeneity in water treatment conditions. Table 5 shows the correlation coefficients between simulated and measured soil moisture in each layer. The correlation coefficients are significant. The simulations were better for deeper layers than for shallow layers, and the simulated average soil moisture of the whole soil profile (0–50 cm) was better than individual layers. That means the model has good capacity to capture the overall water budget, but the water distribution may differ from plot to plot because of the heterogeneity of the soils. In Jiangsu experiments (Case 2), the model has a tendency of underestimating soil moisture (Fig. 5), that is mainly because the water table position is usually high at this site (1–2 m below the surface) and can provide a substantial water to top soil layers. In the model we treat water table as a constant to estimate the soil moisture of the bottom layer. For such high water table conditions, an explicit water table dynamic submodel may be needed in the future development.

4.3.2. Crop growth

Using a set of parameters for a cultivar, Crop-DNDC can simulate the phenological stages well for wheat in Shandong and Jiangsu experiments in different years and different planting dates. The difference between simulated and measured development stages was within 5 days. For the rice experiments in Hunan, simulation errors for the dates of beginning panical initiation, flowering and maturity were within 7 days, and usually are within 2 days, although the planting dates were very different (Table 4).

Crop-DNDC captured the variation patterns of LAI and biomass (Table 5 for Shandong experiments and Fig. 5 for Jiangsu experiments) although several measurements in May 1984 of Jiansu experiments were unusually high. Fig. 6 shows the comparisons between simulated and measured LAI, above ground biomass and plant

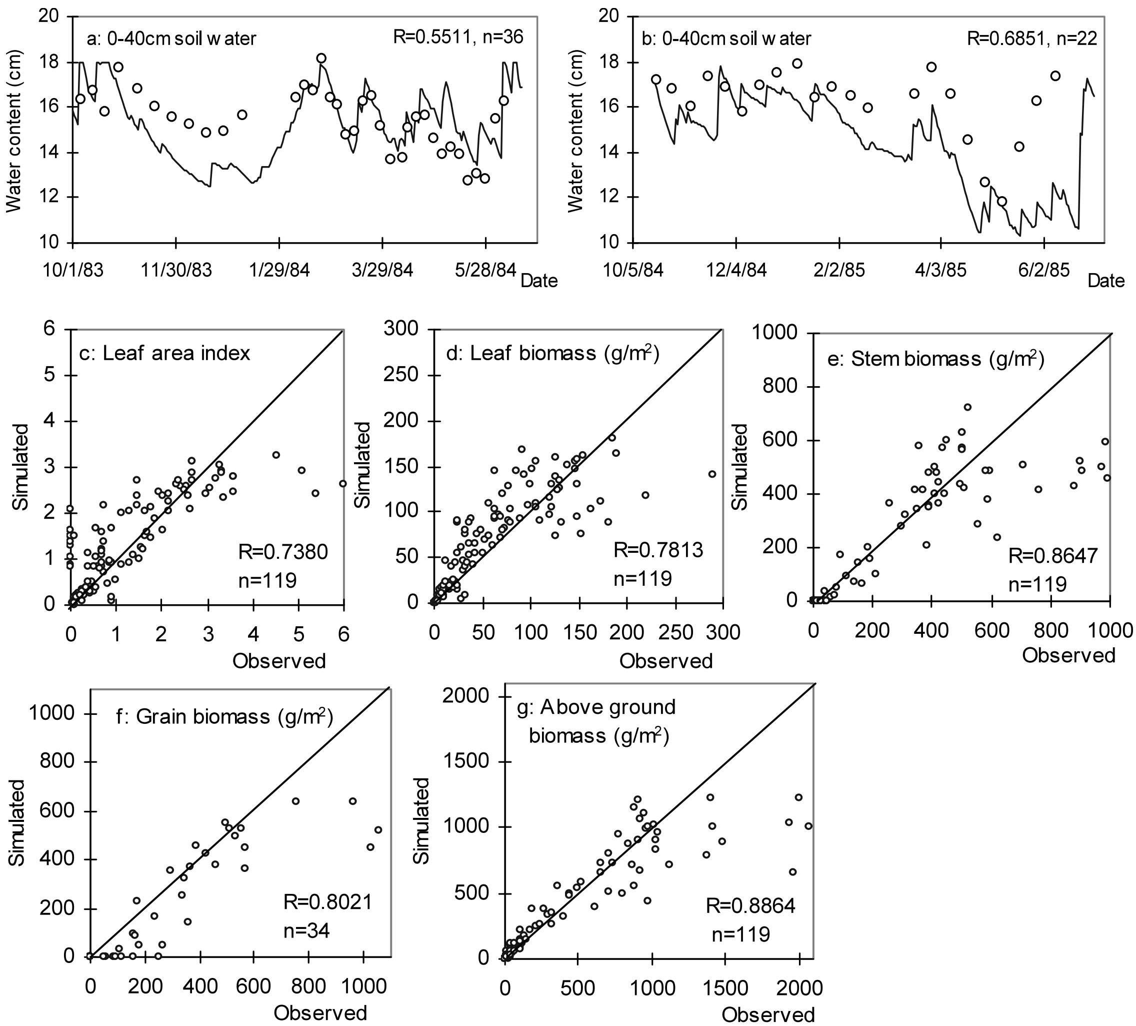

Fig. 5. Comparisons between simulated and measured (a and b) soil water content in 0–40 cm, (c) LAI, (d) leaf biomass, (e) stem biomass and (f) grain biomass for the winter wheat experiments in Jiangsu, China. In graph a and b, curves are for simulated results, circles are for measurements. n is the number of observations and R is the correlation coefficient.

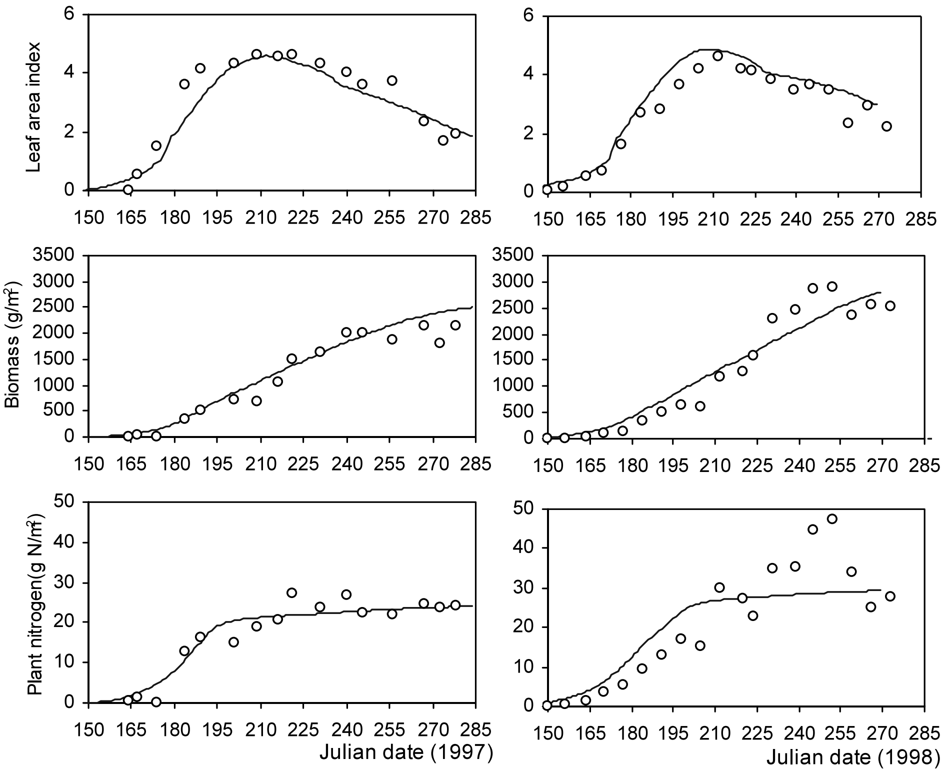

Fig. 6. Comparisons between simulated and measured LAI, above ground biomass and plant nitrogen for the corn experiments in Iowa, USA. Curves are for simulated results, circles are for measurements.

nitrogen for the experiments in Iowa. The simulated variation trends were in agreement with the measurements. LAI, biomass and nitrogen content were lower in 1997 than in 1998 because of the cool and drought effects in 1997 (the annual precipitation in 1997 is 250 mm less than in 1998, and annual mean temperature in 1997 is 2.5 °C lower than in 1998), the model reflected this difference. The model overestimated root biomass for all the 2 years, which may be because root biomass sampling was incomplete. Fig. 7 shows comparisons between simulated and measured LAI and the biomass of each organ in Hunan experiments. The model captured the variation patterns of LAI and biomass, but the coefficients between simulated results and measurements for root biomass and grain were lower than other items. Incomplete sampling may be the reason of over-estimation of root biomass. Grain yield forming is very complex and more sensitive to crop and environmental conditions, that makes the simulation harder comparing to other plant organs. All the plant biomass measurements were destructive samplings that can bring some sampling errors or inconsistency in biomass change.

4.3.3. Soil biogeochemistry and trace gas emissions

Soil biogeochemistry and trace gas emissions are simulated based on DNDC (Li et al., 1992a) which has been validated extensively (Li et al., 1992b, 1994a,b, 1996, 1997; Li, 2000). We run Crop-DNDC for another three cases to validate that the upgraded model still keeps the capacity of DNDC in simulating soil carbon and nitrogen dynamics and trace gas emissions. The three cases are long-term soil carbon experiments in Illinois, USA (Odell et al., 1984), N_2O emission experiments in La Silva, Costa Rica (Crill et al., 2000), and methane emission from rice fields in Texas, USA (Sass et al., 1990, 1991a,b, 1992, 1994; Sigren et al., 1997a,b). The results show that Crop-DNDC can still capture the long-term variation pattern of soil organic carbon, N_2O emissions and the features of methane emissions, such as the timing, approximate magnitude and variation patterns (Zhang, 1999).

5. Application analysis: sensitivity to climate and farming practices

5.1. Impact of climate change and atmospheric CO_2 enrichment on agroecosystems

In the recent decade, estimating possible impacts of climate change and atmospheric CO_2 enrichment on agriculture is an important aspect of model application. There are lots of studies using different kinds of models and climate change scenarios and in different temporal and spatial scales (Adams et al., 1990; Dhakhwa et al., 1997), usually crop yield is the focus of the studies. Crop-DNDC can simultaneously simulate climate, crop growth and soil biogeochemistry and their interactions, therefore it can provide more comprehensive response of agroecosystems to climate warming and atmospheric CO_2 enrichment. We used the experiments in Iowa (Case 4 in Section 4.1) as a baseline for numerical experiments. The climate warming scenarios are assumed as both daily maximum and minimum temperatures increase 2 °C and precipitation is not changed. The scenarios include the combinations of climate warming (T + 2), atmospheric CO_2 doubling ($2 \times CO_2$) and cultivar adjustment (C). It is assumed that CO_2 concentration of $2 \times CO_2$ is 650 ppm because the effects of other greenhouse gases. Warming climate speeds crop development and shortens crop growing duration, therefore it is assumed that a new cultivar will be used which can approximately maintain the silking and maturity dates unchanged under the warming climate scenarios.

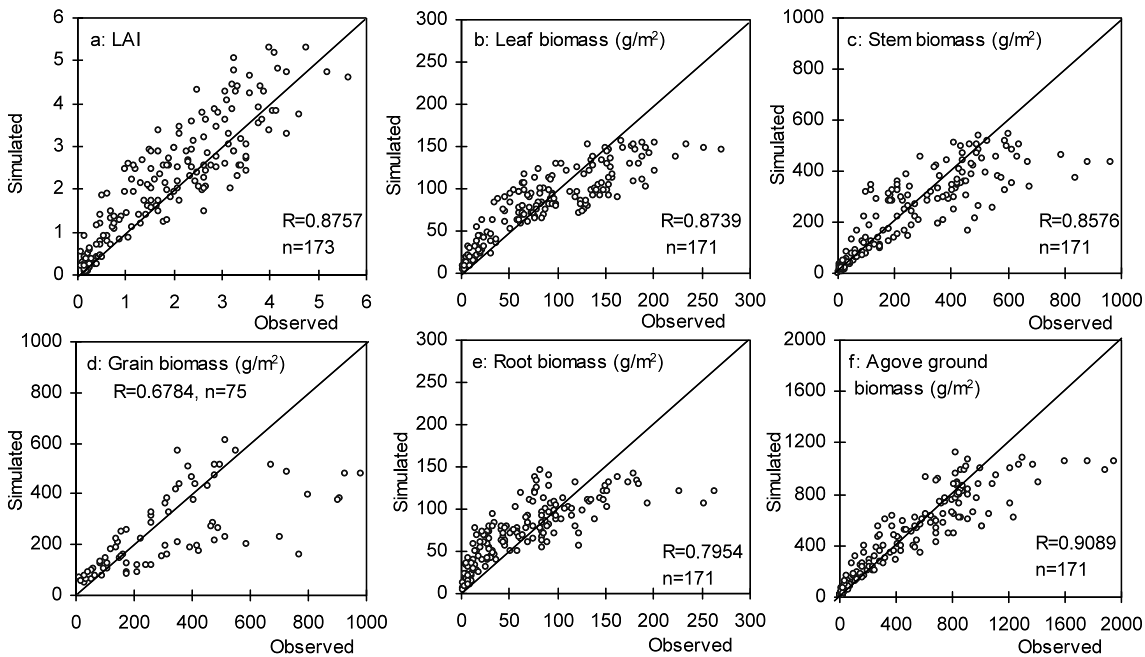

Fig. 7. Comparisons between simulated and measured (a) LAI, (b) leaf biomass, (c) stem biomass, (d) grain biomass, (e) root biomass and (f) above ground biomass for the rice experiments in Hunan, China.

Table 6
Simulation results for the possible effects of climate warming and atmospheric CO_2 enrichment on the agroecosystem

Year	1997				1998			
Scenarios	Base-line	T+2	T+2, $2\times CO_2$	T+2, C, $2\times CO_2$	Base-line	T+2	T+2, $2\times CO_2$	T+2, C, $2\times CO_2$
Total biomass (g/m^2)	2340.4	−5.1%	17.6%	22.4%	2717.9	−7.4%	13.4%	19.7%
Grain yield (g/m^2)	1287.0	−4.3%	12.1%	19.3%	1601.2	−5.8%	1.2%	16.2%
LAI at silking	4.07	0.5%	30.7%	32.9%	4.78	−6.3%	27.8%	35.6%
Silking date	August 12	−7	−7	−2	August 5	−8	−8	−2
Maturity date	October 18	−22	−22	−7	September 26	−16	−16	0
Transpiration (mm)	389.3	−3.3%	0.7%	12.4%	458.7	−10.2%	−4.6%	6.0%
Soil respiration (kg C/ha)	3466.4	21.5%	35.2%	21.4%	5903.6	10.6%	16.9%	11.2%
SOC increase (kg C/ha)	95.9	−254.4	546.8	1106.6	−1436.7	−2496.2	−1056.2	−997.1
N gas loss (kg N/ha)	10.5	30.0%	32.0%	16.0%	22.0	20.1%	12.3%	1.6%
N_2O emission (kg N/ha)	2.7	22.9%	22.2%	20.3%	7.08	−6.8%	−12.6%	−14.7%

Charges are expressed as relative (percentage) or absolute difference comparing to the baseline conditions. T+2 means daily mean temperature increase 2 °C, $2\times CO_2$ is for CO_2 doubling, C is for cultivar adjustment for maintaining an approximately same growing duration.

Table 6 shows the simulation results for the possible impacts of climate warming and atmospheric CO_2 enrichment on the agroecosystem. Significant difference exists between the baseline conditions in 1997 and 1998 because of their weather conditions (drier and cooler in 1997 than in 1998). In 1997, LAI at silking, crop biomass and grain yield, soil respiration, nitrogen gas loss and N_2O emissions were lower than in 1998, and plant matured late mainly because of lower temperature. Crop biomass and grain yield would decrease if daily mean temperature increases 2 °C, which is mainly because higher temperature shortens crop growing duration, doubling can compensate this negative effects, especially in drier and cooler background conditions. By adjusting crop cultivar for an approximately same growing duration as under baseline conditions, crop biomass and grain yield would increase about 20% in the T + 2 plus 2 × CO_2 scenario. High temperature will enhance soil respiration. Annual soil organic carbon balance was positive (SOC increased) under all the scenarios based on 1997 except T + 2, while the balance was negative (SOC decreased) for all the scenarios based on 1998. The effects of the scenarios on N_2O emissions were quite different for different baseline conditions. N_2O emission in 1998 was higher than in 1997 mainly because of the difference in water conditions. The results show that the baseline conditions or the climate variability are important in climate change impact analysis, especially for N_2O emissions and soil carbon balance.

5.2. Managing agroecosystems for sustainable agriculture

Agricultural production should be productive, efficient, long-lasting and environmentally safe.

Balancing all these aspects will be an important issue for modern agriculture. According to the functions of the Crop-DNDC model, we quantify the following factors for the consideration of sustainable agriculture:

- productivity—grain yield, crop total biomass and economic benefit;
- efficiency—water use efficiency, and nitrogen use efficiency;
- long-lasting—soil organic carbon accumulation;
- environment implications—emissions of greenhouse gases and other atmospherically active gases (e.g., NO and NH_3), and nitrate leaching.

We conducted numerical experiments based on the weather and soil conditions in Iowa in 1997 (Case 4 in Section 4.1). The management treatments included sowing date (10 days later than the normal), removing the straws after harvest, nitrogen input amount (100, 200, 300 and 400 kg N/ha), nitrogen fertilizer types (NO_3^-, NH_4^+, urea, HN_3 and manure), fertilization dates (June 11, July 11, August 10, September 9), water amount used for irrigation (50, 100 and 150 mm) and irrigation dates (June 11, July 11 and August 10). It was assumed that fertilizer or manure is applied on the soil surface, and the C/N ratio of the manure was 30 (the manure input is 3000 kg C/ha for 100 kg N/ha nitrogen). The economic benefit is the difference between the income from the grain yield and the costs of management. We assumed the prices were grain is \$0.07/kg, fertilizer is \$0.5/kg N; irrigation is \$1/mm/ha, operation cost for irrigation and fertilization is \$10 for each time, the cost of planting plus harvesting is \$50/ha. Water use efficiency here is defined as the ratio of crop biomass (kg/ha) to annual water input (precipitation and irrigation in mm). Nitrogen use efficiency is defined as the ratio of crop nitrogen uptake to available N in soil (fertilization and mineralization). Nitrogen use efficiency may be slightly larger than one because crop takes up some mineral nitrogen that initially existed in soil. Nitrogen loss includes nitrate leaching and nitrogen gas emissions. Total greenhouse gas emission from crop–soil systems includes CO_2 (the difference between soil respiration and crop assimilation) and N_2O emissions. We assume 1 kg N_2O is equivalent to 270 kg CO_2 in greenhouse effects (Albritton et al., 1995). Nitrate leaching here is defined as the nitrate downward flux at the depth of 1 m.

The results show that different treatments have different effects on productivity, efficiency, soil organic carbon and environment implications (Table 7). For example, using fertilizers increases crop biomass and grain yield, but the economic benefit decreases when fertilizer input is too high. With the increase in nitrogen input, crop nitrogen use efficiency decreases and nitrogen gas emissions (especially N_2O emissions) and nitrogen loss increase, but soil organic carbon increase because of the increase of crop biomass. Greenhouse gas emissions decrease when fertilization is moderate, but increase when fertilization is very high (400 kg N/ha), because of the dramatic increase of N_2O emissions. Irrigation can promote the downward flow and leaching of mineral nitrogen, and increase nitrogen stress (especially for early irrigation), because the stress of nitrogen is more serious than the stress of water. Obviously these results are very much dependant on the specific conditions and scenarios assumed, but these numerical experiments show that Crop-DNDC provides a framework to quantify and evaluate the effects of management practices on the various aspects of agricultural ecosystem. It exhibits the potential of the model applications in optimizing management strategies by compromising our economic and environmental requirements, and balancing our current and long-term benefits.

6. Conclusions

This paper describes the development of a processes-oriented model, which combined crop growth with soil biogeochemical processes, and hence is able to predict both crop and soil dynamics simultaneously. Validation analysis showed that the model is able to capture the patterns of soil moisture, crop growth and soil carbon and nitrogen dynamics. Application analysis exhibits the sensitivity of the model to climate conditions, atmospheric CO_2 concentration and various farming practices. That shows the potential application

Table 7
Numerical experiments for the effects of farming practices on productivity, efficiency, soil organic carbon and environmental implications

Farming practice		Productivity (increase (%))			Use efficiency[a]			SOC increase (kg C/ha)	Environmental implications				
		Biomass	Yield	Benefit	Water	N	N loss (kg N/ha)		CO_2 emissions (t/ha)[b]	Leaching (kg N/ha)	N_2O emissions (kg N/ha)	NO emissions (kg N/ha)	NH_3 emissions (kg N/ha)
Baseline (no treatment)		0.0	0.0	0.0	32.9	1.17	6.6	−720.3	−11.6	2.2	0.7	0.3	2.7
Sowing 10 days later		−1.9	−2.6	−2.9	32.3	1.20	6.8	−727.3	−11.2	2.3	0.7	0.3	2.8
Removing the straws		0.0	0.0	0.0	32.9	1.18	6.3	−2931.1	−11.8	2.2	0.7	0.3	2.5
N amount	100	18.8	23.1	17.6	39.1	0.88	7.4	−199.6	−16.8	2.2	1.0	0.3	3.2
(NO_3^-, kg N/ha, May 12)	200	34.4	44.1	33.0	44.1	0.78	12.7	95.9	−19.8	2.2	2.7	0.3	3.5
	300	49.8	59.9	42.5	49.3	0.70	18.5	555.0	−20.6	2.3	11.0	0.3	4.1
	400	57.8	60.9	35.7	51.9	0.66	31.7	626.2	−16.4	2.3	22.0	0.4	5.6
N type	NH_4^+	22.2	27.5	22.6	40.2	0.94	28.1	−124.9	−17.7	2.2	1.0	1.2	23.4
(100 kg N/ha, May 12)	Urea	21.0	25.9	20.8	39.8	0.92	34.8	−148.6	−17.4	2.2	0.9	0.6	30.5
	NH_3	19.4	23.6	18.3	39.3	0.90	41.6	−175.7	−17.0	2.2	0.8	0.6	37.1
	Manure	8.9	10.8	4.0	35.8	1.05	10.1	1448.9	−10.1	2.2	0.7	0.3	5.6
N date	June 11	30.2	38.9	35.3	42.8	1.08	7.18	12.1	−19.9	2.2	0.9	0.3	3.0
(NO_3^-, 100 kg N/ha)	July 11	28.5	38.4	34.7	42.3	1.08	6.7	−90.5	−19.4	2.2	0.8	0.3	2.6
	August 10	17.9	30.4	25.8	38.8	1.05	7.3	−454.6	−16.3	2.2	1.5	0.3	2.6
	September 9	14.3	22.7	17.2	37.6	1.04	7.2	−692.8	−14.9	2.2	0.9	0.3	3.0
Irrigation	50	−3.3	−2.7	−11.0	29.3	1.13	8.4	−868.2	−10.6	3.6	0.8	0.3	3.0
Amount (mm, May 12)	100	−14.2	−14.2	−31.8	24.1	0.96	11.1	−1272.5	−7.4	5.8	0.9	0.3	2.5
	150	−13.5	−13.6	−39.1	22.6	0.98	12.1	−1242.3	−7.6	6.8	0.9	0.3	2.6
Irrigation date (100 mm)	June 11	−4.9	−4.2	−20.7	26.6	1.09	9.5	−1078.4	−9.6	4.5	0.9	0.3	2.6
	July 11	0.6	1.7	−14.1	28.2	1.16	6.6	−936.2	−11.1	2.2	0.7	0.3	2.6
	August 10	−0.5	−0.3	−16.3	27.9	1.09	6.9	−1358.4	−9.2	2.2	0.8	0.3	2.6

[a] Water use efficiency is defined as the ratio of crop biomass (kg/ha) to annual water input (precipitation and irrigation in mm). Nitrogen use efficiency is the ratio of crop nitrogen uptake to the sum of annual fertilization and mineralization.

[b] Emission of greenhouse gases to the atmosphere from crop–soil system (CO_2 equivalent, Ton CO_2/ha).

of the model in researches and policy-makings relating to climate change, greenhouse gas mitigation and sustainable agriculture.

In comparison with several existing crop growth models and soil biogeochemical models (Table 8), the Crop-DNDC model has two major advantages: it integrates crop growth and soil biogeochemistry, and can be used for predicting impacts of climate change or alternative management on both agricultural production and envi-

Table 8
A comparison of Crop-DNDC with other models 1998

	Crop-DNDC	CERES[a]	GePSi[b]	RothC[c]	CENTURY[d]	DNDC[e]	*ecosys*[f]
General features of the models							
Time step	Daily	Daily	Hourly	Monthly	Monthly	Daily	Hourly
Simulation period (years)[g]	10^{0}–10^{2}	10^{0}–10^{1}	10^{0}–10^{1}	10^{0}–10^{2}	10^{0}–10^{2}	10^{0}–10^{2}	10^{-1}–10^{0}
Plant pools	4	4	5	0	3	2	>50
Soil organic C pools	8	4	0	5	8	8	~40
Soil inorganic N pools	7	2	2	0	2	7	1
Processes explicitly simulated in the models							
Soil temperature	√	√	√	√	√	√	√
Soil moisture	√	√	√	√	√	√	√
Phenology	√	√	√				
LAI	√	√	√				√
Photosynthesis	√	√	√				√
Respiration	√	√	√				√
Rooting processes	√	√	√				√
N uptake	√	√	√		√	√	√
Water effects on crop	√	√	√		√		√
N effects on crop	√	√	√		√	√	√
CO_2 effects on crop	√		√				√
Decomposition	√	√		√	√	√	√
CH_4 emissions	√						√
Mineralization	√	√	√		√	√	√
Nitrification	√		√		√	√	
Denitrification	√		√		√	√	
N trace gas emissions	√				√	√	
Primary output of the models							
Soil temperature	√	√	√		√	√	√
Soil moisture	√	√	√		√	√	√
Phenological stages	√	√	√				
LAI	√	√	√				√
Plant C pools	√	√	√		√	√	√
Plant N pools	√	√	√		√	√	√
Soil C pools	√			√	√	√	√
Soil N pools	√	√	√		√	√	√
CH_4 emissions	√						√
N trace gas emissions	√					√	

[a] Ritchie et al., 1988, 1987; Jones and Kiniry, 1986.
[b] Chen and Reynolds, 1997.
[c] Jenkinson, 1990.
[d] Parton et al., 1988.
[e] Li et al., 1992a.
[f] Grant, 1998. Other related publications about *ecosys* can be found in its references.
[g] General time period for model validation and application.

ronmental safety. In the widely used CERES models (Ritchie et al., 1988, 1987; Jones and Kiniry, 1986), crop photosynthesis is estimated based on empirical equations, and soil biogeochemical processes are simulated simply for the purpose of crop nitrogen stress. The CERES models cannot be used for either trace gas emissions or long-term soil carbon dynamics. GePSi (Chen and Reynolds, 1997) simulates canopy microclimate conditions, soil physical processes and plant growth, but there are less considerations about soil carbon dynamics and trace gas emissions. And some other crop models, such as RCSOD (Gao et al., 1992) and ORIZA1 (Kropff and van Laar, 1993), do not consider soil biogeochemical processes at all. The RothC model (Jenkinson, 1990) focuses on soil carbon turnover using plant residue as input. Crop growth and trace gas emissions are not included in the model. Both CENTURY (Parton et al., 1988) and DNDC (Li et al., 1992a) estimate crop biomass (C and N) empirically, therefore they cannot well reflect the effects of climate conditions and farming practices on crop growth, especially for the purpose of food production. The *ecosys* model (Grant, 1998) simulates crop physiological processes and soil biogeochemistry in more detailed schemes and at a finer scale. The model is much complex and requires more input data. Crop-DNDC integrates crop growth and soil biogeochemical processes, and considers practical applications. It can be used to assess the effects of climate change or alternative management on crop yield, soil carbon sequestration and trace gas emissions.

Acknowledgements

The authors are indebted to Shunqing An, Futang Wang and Michael Keller for providing us unpublished data for validating the model. Xianming Xiao gave us lots of help in processing weather data. The editor and two anonymous reviewers provided important comments which significantly improved the quality of this paper. This study was jointly supported by the Chinese National Foundation of Natural Science (grant No. 49899270), the US Natural Science Foundation's TECO-Program and the National Aeronautic and Space Administration (NASA) through project 'Atmospheric Impacts of Agriculture'.

Appendix A. Equations of the Crop-DNDC model

Equations	Description
Day length and soar radiation	
$\mathrm{DL} = 12 + 24/\pi \arcsin S/C$	Day length
$S = \sin\varphi \sin\omega$	
$C = \cos\varphi \cos\omega$	
$\omega = -\arcsin[\sin(23.4 \times 180/\pi)\cos(2\pi(\mathrm{JD} + 10)/365)]$	Solar declination
$\mathrm{SR_d} = \mathrm{DS_0}(a + b\mathrm{Sh}/\mathrm{DL})$	Deriving solar radiation from sunshine duration
$\mathrm{SR_d} = \mathrm{DS_0} 0.7[1 - \exp(-B\Delta T^{24})]$	Deriving solar radiation from temperature extremes

Equations	Description
$DS_0 = 3600SC[DLS + 24C(1 - S^2/C^2)^{0.5}/\pi]$	Extraterrestrial insolation
$SC = 1370[1 + 0.033\cos(2\pi JD/365)]$	Solar constant
$I_0 = 0.55SR_d(\sin\beta)(1 + 0.4\sin\beta)/x$	Photosynthetically active radiation at certain time
$x = 3600[DL(S + 0.4S^2 + 0.2C^2) + 12C(2 + 1.2SL\pi(1 - S^2/C^2)^{0.5})]$	
$\sin\beta = S + C\cos[2\pi(t + 12)/24]$	Sine of solar elevation
Temperature	
$T_{c\,max} = T_{max}f_s(T_{max})$	Canopy daily maximum temperature
$T_{c\,min} = T_{min}f_s(T_{min})$	Canopy daily minimum temperature
$f_s(T) = \begin{cases} 1 & \text{when } T \geq 0 \\ 2 + T[0.4 + 0.0018(\min(15, \text{Snow}) - 15)^2] & \text{when } T < 0 \end{cases}$	Effects of snow cover on canopy temperature
$T_{cm} = 0.5T_{c\,max} + 0.5T_{c\,min}$	Canopy daily mean temperature
$T_{cd} = 0.5T_{cm} + 0.5T_{c\,max}$	Canopy daytime mean temperature
$T_c(t) = T_{c\,min} + (T_{c\,max} - T_{c\,min})\sin[\pi(t - 11.82 + 0.5DL)/(DL - 3.3)]$ Daytime	Canopy hourly temperature during daytime
$T_c(t) = T_{c\,min} + (T' - T_{c\,min})\exp[2\pi(t - 11.82 + 0.5DL)/(24 - DL)$ Nighttime	Canopy hourly temperature during nighttime
$T_{sl} = T_{am} + \exp(-2/DD)[DT + 0.5T_{aa}\cos(2\pi(JD - JD_0)/365 - 2/DD)]$	Daily mean temperature of soil layers
$DT = \sum_{k=1}^{5} 0.2T_k - [T_{am} + 0.2T_{aa}\cos(2\pi(JD - H)/365)]$	Surface temperature adjustment factor
$T_k = (1 - \alpha)[T_{cm} + (T_{c\,max} - T_{c\,min})(0.03SR_d)^{0.5} + \alpha T_{k+1}]$	Estimated soil surface temperature

Equations	Description
$DD = x_1 \exp[\ln(50/x_1)((1-x_2)/(1+x_2))^2]$	Damping depth (cm)
$x_1 = 100+250BD/(BD+\exp(5.63-5.63BD))$	
$x_2 = SW_l/(3.65-1.44BD_l)$	
Water	
$SM_{max} = 0.07T_{cm}$	Daily maximum snow melt (cm)
$PI_{max} = 0.02LAI$	Daily maximum crop interception (cm)
$\text{Runoff} = \begin{cases} 0.1(w-0.2s)^2/(w+0.8s) & \text{when } w \geq 0.2s \\ 0 & \text{when } w < 0.2s \end{cases}$	Daily surface runoff (cm)
$s = 254(100-cn)/cn$	Retention factor
$\text{Drain} = SW_{con}(SW_l - FC_l)H_l$	Daily gravitational redistribution from layer l to $l+1$
$\text{Diff} = D_w(\theta_l - \theta_{l-1})/(H_l + H_{l-1})0.5H_l$	Daily matric redistribution rate from layer 1 to $l-1$
$D_w = 0.88 \exp[35.4 \times 0.5(\theta_l + \theta_{l-1})]$	Diffusion coefficient
$\theta_l = SW_l - LL_l$	
$ET_p = \begin{cases} 0.01E_{EQ}\exp[0.18(T_{c\ max}+20)] & \text{when } T_{c\ max} < 5 \\ 1.1E_{EQ} & \text{when } 5 \leq T_{c\ max} < 24 \\ E_{EQ}(1-0.43LAI) & \text{when } T_{c\ max} \geq 24 \end{cases}$	Potential evapotranspiration
$E_{EQ} = 0.0001\ SR_d(4.88-4.37\alpha)(T_{cd}+29)$	Equilibrium evapotranspiration
$\alpha = \begin{cases} 0.6 & \text{Snow} > 0.5 \\ \alpha_0 & \text{No crop} \\ 0.23+(LAI-4)^2/160 & \text{Grain filling stage} \\ 0.23-(0.23-\alpha_0)\exp(-0.75LAI) & \text{Others} \end{cases}$	

Equations	Description
$E\mathrm{p} = \begin{cases} \mathrm{ET_p}/1.1\exp(-0.4\mathrm{LAI}) & \text{when} \quad \mathrm{LAI} \geq 1 \\ \mathrm{ET_p}(1-0.43\mathrm{LAI}) & \text{when} \quad \mathrm{LAI} < 1 \end{cases}$	Potential evaporation
$T_\mathrm{p} = \mathrm{ET_p} - E_\mathrm{p}$	Potential transpiration
$E_\mathrm{a} = E_\mathrm{p} f_\mathrm{D,E}$	Actual soil evaporation
$f_\mathrm{D,E} = \sum_{l=0}^{\mathrm{ne}} (\mathrm{SW}_l - \mathrm{LL}_l)/(\mathrm{FC}_l - \mathrm{LL}_l) H_l / Z_\mathrm{ne}$	Effects of soil moisture on evaporation
$T_\mathrm{a} = \min\left(T_\mathrm{p}, \sum_{l=0}^{n} \mathrm{Wup}_l\right)$	Actual transpiration
$\mathrm{Wup}_l = R_0 \mathrm{Rld}_l/(0.2+0.2\mathrm{Rld}_l) f_{\mathrm{w1},l} H_l$	Crop uptake capacity from layer l
$f_{\mathrm{w1},l} = \sin[(\mathrm{SW}_l - \mathrm{LL}_l)/(\mathrm{FC}_l - \mathrm{LL}_l)1.25\pi/2]$	Effects of soil moisture on water uptake
$\mathrm{ws} = T_\mathrm{a}/T_\mathrm{p}$	Crop water stress factor
Photosynthesis	
$P_0 = 0.1 \times 30/44 \min(\mathrm{ws,ns}) f_\mathrm{CO2} \sum_{i=1}^{3} \sum_{j=1}^{3} P(L_i,t_j) \mathrm{LAI\ DL} w_{2j} w_{2i}$	Daily gross photosynthesis (g/m^2)
$f_\mathrm{CO2} = 1 + \mu \ln(\mathrm{CO_2}/340)$	Effects of CO_2 concentration on photosynthesis
$L_i = \mathrm{LAI}.w_i \quad (i = 1,2,3)$	Three canopy layers for Gaussian integration
$t_j = 12 + 0.5\mathrm{DL}.w_j \quad (j = 1,2,3)$	Three points of time for Gaussian integration
$P(L_i,t_j) = F_\mathrm{SL} P_\mathrm{SL} + (1 - F_\mathrm{SL}) P_\mathrm{SH}$	Gross photosynthesis rate at layer L_i and time t_j
$F_\mathrm{SL} = \exp(-K_\mathrm{BL} L_i)$	Fraction of sunlit leaf area
$P_\mathrm{SH} = \mathrm{Am}[1 - \exp(-I_\mathrm{SH} E/\mathrm{Am})]$	Photosynthesis rate of sunlit leaves

Equations	Description
$P_{SL} = \text{Am}[1-(\text{Am}-P_{SH})[1-\exp(-I_{PDR}E/\text{Am})]/(I_{PDR}E)]$	Photosynthesis rate of shaded leaves
$\text{Am} = A_{\max_0} f_{TP}$	Photosynthesis at light saturation
$I_{PDR} = (1-\sigma)I_{DR0}/\sin\beta$	Light which is perpendicular to leaf surface
$I_{SH} = I_{DF} + (I_{DR} - I'_{DR})$	Light absorbed by shaded leaves in a layer
$I_{DF} = (1-\alpha_h)I_{DF0}K_{DF}\exp(-K_{DF}L_i)$	Diffuse light
$I_{DR} = (1-\alpha_s)I_{DR0}K_{DR}\exp(-K_{DR}L_i)$	Direct light
$I'_{DR} = (1-\sigma)I_{DR0}K_{BL}\exp(-K_{BL}L_i)$	Direct component of the direct light after canopy scattering
$\alpha_h = [1-(1-\sigma)^{0.5}]/[1+(1-\sigma)^{0.5}]$	Reflectivity of horizontally distributed canopy
$\alpha_s = 2\alpha_h/(1+2\sin\beta)$	Reflectivity of spherically distributed canopy
$K_{BL} = 0.5K_{DF}/[0.8\sin\beta(1-\sigma)^{0.5}]$	Extinction coefficient of assumed black body leaves
$K_{DR} = K_{BL}(1-\sigma)^{0.5}$	Extinction coefficient of direct light
$I_{DR0} = I_0 - I_{DF0}$	Direct light above the canopy
$I_{DF0} = I_0 F_{DF}$	Diffuse light above the canopy
$F_{DF} = \begin{cases} 1 & \text{when } C_{at} \le 0.22 \\ 1-6.4(C_{at}-0.22)^2 & \text{when } 0.22 < C_{at} \le 0.35 \\ 1.47-1.66C_{at} & \text{when } 0.35 < C_{at} \le x_3 \\ x_4 & \text{when } C_a > x_3 \end{cases}$	Fraction of diffuse light above the canopy
$x_4 = 0.847 - 1.61\sin\beta + 1.04\sin^2\beta$	
$x_3 = (1.47 - x_4)/1.66$	

Equations	Description
$C_{at} = I_0(0.5\text{SC} \sin \beta)$	Atmospheric transmission coefficient
Respiration	
$R_{mk} = R_{m0k} Q_{10}^{(T_{cm}-25)/10} \text{BM}_k$	Maintenance respiration
$R_g = \left(P_0 - \sum_{k=1}^{4} R_{mk}\right)(1 - 1/R_{g0})$	Growth respiration
Rooting	
$\Delta D_{root} = 0.2\text{Dtt} \min(\text{RT}_S, \text{RT}_A)$	Daily increase of root front depth
$\Delta \text{Rld}_l = R\text{Asm}(1-F)/H_l f_{\text{ROOT}_l} / \sum_{i=1}^{n} f_{\text{ROOT}_i} - \text{Rld}_l F_{\text{RS}l}$	Daily increase of root length density in layer l
$R = \sum \text{Rld}_l H_l / \text{BM}_{\text{Root}}$	Average specific root length
$f_{\text{ROOT}_l} = [1 - Z_l/300]^{\text{CP Root}} \min(\text{RT}_S, \text{RT}_A, \text{RT}_T, \text{RT}_N)$	Root distribution factor
$F_{\text{RS}l} = 0.01(2 - \min(\text{RT}_S, \text{RT}_A, \text{RT}_T, \text{RT}_N))$	Fraction of daily root senescence
$\text{RT}_S = \frac{1.6 + 0.4\text{sand}_l - \text{BD}_l}{0.5 - 0.1\text{sand}_l} \sin\left(1.25 \frac{\text{SW}_l - \text{LL}_l}{\text{FC}_l - \text{LL}_l} \frac{\pi}{2}\right)$	Soil strength limiting factor
$\text{RT}_A = \text{CP}_{\text{WET}} + (1 - \text{CP}_{\text{WET}})(\text{UL} - \text{SW}_l)/(\text{UL} - \text{FC}_l)$	Soil aeration limiting factor
$T_T = \cos(\pi(T_s - 20)/40)$	Soil temperature limiting factor
$\text{RT}_N = 1 - 1.17 \exp[-0.15(\text{NO}_{3pl} + \text{NH}_{4pl})]$	Soil nitrogen limiting factor
Crop nitrogen	
$N_{\text{dem}} = N_{\text{dem, d}} + N_{\text{dem, g}}$	Daily nitrogen demand
$N_{\text{dem, d}} = \text{BM}_{\text{Root}}(N_{\text{R0}} - N_{\text{R}}) + (\text{BM}_{\text{Leaf}} + \text{BM}_{\text{Stem}})(N_{\text{S0}} - N_{\text{S}})$	Deficiency demand
$N_{\text{dem, g}} = \text{Asm}[F.N_{\text{S0}} + (1-F)N_{\text{R0}}]$	Growth demand

Equations	Description
$\mathrm{Nup}=0.06\sum f_{\mathrm{W2},l}\mathrm{Rld}_l(f_{\mathrm{NO3}l}+f_{\mathrm{NH4}l})H_l$	Uptake capacity
$f_{\mathrm{NO3}l}=1-\exp(-0.0275\mathrm{NO}_{3pl})$	Effects of nitrate concentration
$f_{\mathrm{NH4}l}=1-\exp(-0.0275\mathrm{NH}_{4pl})$	Effects of ammonium concentration
$f_{\mathrm{W2},l}=1-0.5(\mathrm{SW}_l-\mathrm{LL}_l)/(\mathrm{FC}_l-\mathrm{LL}_l)$	Effects of soil moisture
$\mathrm{ns}=1-(N_{\mathrm{S}}-N_{\mathrm{S0}})/(N_{\mathrm{S0}}-N_{\mathrm{S\ min}})$	Nitrogen stress factor
$N_{\mathrm{pool}}=[\mathrm{BM}_{\mathrm{Root}}(N_{\mathrm{R}}-N_{\mathrm{R\ min}})+(\mathrm{BM}_{\mathrm{Leaf}}+\mathrm{BM}_{\mathrm{Stem}})(N_{\mathrm{S}}-N_{\mathrm{S\ min}})](0.15+0.5\mathrm{ns})$	Movable nitrogen in shoot and root
Decomposition and methane emissions	
$\Delta C_i=\mu_{\mathrm{clay}}\mu_{\mathrm{CN}}\mu_{\mathrm{T}}\mu_{\mathrm{W}}\mu_{\mathrm{Til}}K_{\mathrm{C}i}C_i$	Decomposition rate of a carbon pool
$\mu_{\mathrm{T}}=0.2161+0.093T_{\mathrm{s}}-0.0014T_{\mathrm{s}}^2$	The effects of temperature
$\mu_{\mathrm{W}}=-1.7827W_{\mathrm{fps},\ l}^2+2.3824W_{\mathrm{fps}}-0.222$	The effects of moisture
$\mu_{\mathrm{clay}}=\log(0.14/\mathrm{clay}_l)+1$	The effects of clay adsorption
$\mathrm{Aere}=\mathrm{BM}_{\mathrm{root}}/1000$ Rice	Aerenchyma factor
$\Delta\mathrm{Ch}_l=\begin{cases}100(0.5\mathrm{Aere}-0.5) & \text{Flooding}\\ 100[0.5\mathrm{Aere}+100(1-W_{\mathrm{fps}\ l})] & \text{Nonflooding}\end{cases}$	Daily increase of redox potential
$\mathrm{CH}_{4\mathrm{E}}=\mathrm{CH}_{4\mathrm{P}}-\mathrm{CH}_{4\mathrm{O}}$	Daily methane emissions to the atmosphere
$\mathrm{CH}_{4\mathrm{O}}=\mathrm{CH}_{4\mathrm{P}}(0.5+0.5\mathrm{Aere})$	Daily methane oxidation
$\mathrm{CH}_{4\mathrm{P}}=0.47C_{\mathrm{CH4}}f_{\mathrm{TM}}f_{\mathrm{Eh}}f_{\mathrm{pHM}}$	Daily methane production

Equations	Description
$C_{CH4}=\sum_{l=0}^{n}[C_{Sl}+F_{RSl}F_{ROOT/}BM_{Root}4]$	Carbon pool for methane production
$f_{TM}=\exp[0.33(T_s-23)]/[1+\exp(0.33(T_s-23))]$	Effects of temperature
$f_{Eh}=\begin{cases}1 & Eh\leq -200\\ 0 & Eh>-200\end{cases}$	Effects of redox potential
$f_{pHM}=\frac{(pH-5.5)(pH-9.0)}{(pH-5.5)(pH-9.0)-(pH-7.5)^2}$	Effects of pH
Soil nitrogen	
$F_{NH4}=[0.41-0.47\log(NH_4)clay/clay_{max}$	Ammonium adsorption
$\log K_{NH4}-\log K_{H2O}=\log(NH_{4m}/NH_{3m})+pH$	Equilibrium of ammonium and ammonia
$AM=2NH_3(D_{NO3,N}t/3.14)^{0.5}$	Ammonia volatilization
$NO_{3,N}=NH_4[1-\exp(-K_{35}f_{TN})]f_{WN}f_{pH,N}$	Nitrification rate
$f_{T,N}=-0.0272(0.1T_s)^4+0.1566(0.1T_s)^3-0.2234(0.1T_s)^2+0.03094T_s-0.0233$	Effects of temperature on nitrification
$f_{W,N}=-12.904W_{fps}^4+17.651W_{fps}^3-5.5368W_{fps}^2+0.9975W_{fps}-0.0243$	Effects of soil moisture on nitrification
$f_{pH,N}=-0.0604pH^2+0.7347pH-1.2314$	Effect of pH on nitrification
$J_s=-SW_lD_SG_S+J_wS_C$	Solute movement
$D_S=0.6+2.93v^{1.11}$	Diffusion coefficient
$\mu_{T,DN}=2^{(T_S-22.5)/10}$	Temperature reduction factor
$\mu_{pH,NO3}=0.313(pH-3.18)$	pH reduction factor

Equations	Description
$\mu_{pH,NO2}=1.0$	pH reduction factor
$\mu_{pH,\ NO2}=0.384(pH-4.4)$	
$(dB/dt)_g=U_{DN}B(t)$	Denitrifier growth rate
$U_{DN}=\mu_{T,DN}(U_{NO3}\mu_{pH,\ NO3}+U_{NO2}\mu_{pH,\ NO2}+U_{N2O}\mu_{pH,\ N2O})$	Relative denitrifier growth rate
$U_{NxOy}=U_{NxOy,\ m}C_s/(K_{c,\ 1/2}+C_s)NxOy/(K_{NxOy,\ 1/2}+NxOy)$	Maximum denitrifier growth rate
$(dB/dt)_d=M_cY_cB(t)$	Denitrifier death rate
$C_{CON}=(U_{DN}/Y_c+M_c)B(t)$	Consumption of soluble carbon
$CO_{2,\ DN}=C_{CON}-(dB/dt)_g$	CO_2 production
$dNxOy/dt=(U_{NxOy}/Y_{NxOy}+M_{NxOy}NxOy/N)B(t)\mu_{pH,\ NxOy}\mu_{T,DN}$	Nitrate, nitrite, and nitrous oxide consumption
$(dN/dt)asm=(dB/dt)g1/CNR_{DN}$	Nitrogen assimilation rate
$N_2O_N=0.0006NO_{3.N}W_{fps}2.72^{34.6-9615/(T_s+273.15)}$	N_2O production during nitrification
$NO_N=0.0025NO_{3,N}2.72^{34.6-9615/(T_s+273.15)}$	NO production during nitrification
$F_{N2O,NO}=0.017+(0.025-0.0013f_{clay})(1-W_{fps})2^{T_s/20}$	N_2O and NO emissions
$F_{N2}=(0.0006+0.0013f_{clay})+(0.013-0.005f_{clay})(1-W_{fps})2^{T_s/20}$	N_2 emissions

Appendix B. Notation

Symbol	Notation
a	Empirical parameter, 0.25, 0.29 and 0.18 for dry tropical, wet tropical and other areas, respectively
Aere	Plant aerenchyma factor
Am	Photosynthesis rate at light saturation (kg CO_2/ha/h)
AM	Accumulated NH_3 loss at time t (kg N/ha)
A_{max0}	Photosynthesis rate at light saturation when temperature is optimal (kg CO_2/ha/h, input)
Asm	Daily crop assimilation rate (P_0-R_g, g/m^2)

b	Empirical parameter. 0.45, 0.42, 0.55 for dry tropical, wet tropical and other areas, respectively
B,$B(t)$	Total biomass of denitrifier (kg C/ha)
BD, BD_l	Average soil bulk density of the whole profile, and soil layer l, respectively (g/cm^3)
BM_k	Biomass of crop organ k (g/m^2)
BM_{Leaf}, BM_{Root}, BM_{Stem}	Biomass of leaf, root and stem, respectively (g/m^2)
BM_{Stem0}	Stem biomass at flowering (g/m^2)
C_{at}	Atmospheric transmission coefficient
C_{CH4}	Carbon pool for methane production (kg C/ha)
C_{con}	Consumption of soluble carbon during denitrification (kg C/ha)
CH_{4E}	Emission of methane into the atmosphere (kg C/ha)
CH_{4O}, CH_{4P}	Oxidation and production of methane, respectively (kg C/ha)
C_i, ΔC_i	Carbon pool i and its daily decomposition rate in a layer (kg C/ha)
$clay_l$, $clay_{max}$	Fraction of clay (<0.002 mm) in layer l and maximum clay faction (0.63), respectively
CO_2	Atmospheric CO_2 concentration (ppm)
$CO_{2,DN}$	CO_2 production during denitrification (kg C/ha)
cn	SCS curve number for surface runoff
CNR_{DN}	C/N ratio of denitrifiers (3.45)
C_S, C_{Sl}	Soluble carbon in current layer or in layer l (kg C/ha)
CP_{WET}	Crop parameter, sensitivity to wetting conditions (0.5 for wheat and corn, 1 for rice)
CP_{Root}	Crop parameter for root distribution (2 for wheat and rice, 3 for corn)
$(dB/dt)_g$	Potential growth rate of denitrifier biomass (kg C/ha/h)
$(dB/dt)_d$	Death rate of denitrifier biomass (kg C/ha/h)
$(dN/dt)_{asm}$	Nitrogen assimilation rate by denitrifiers (kg N/ha/h)
DD	Damping depth in soil temperature estimation (cm)
Diff	Daily diffusion flux of water between soil layers (cm)
DL, DL_0	Day length and critical day length for photoperiodism, respectively (h)
D_{crop0}, D_{crop}	Plant density ($plants/m^2$) and stem density ($stems/m^2$), respectively
D_{root}	Depth of root front (cm)
DR	Crop development rate (d^{-1})
Drain	Daily water draining flux (cm)
D_s	Diffusion coefficient of a solute (cm soil ha/kg/d)
DS_0	Extra-terrestrial insolation ($J/m^2/d$)
Dtt	Daily thermal time (°C d)
DT	Adjustment factor for the effects of surface temperature
D_w	Diffusion coefficient of soil water
E	Initial light use efficiency (kg CO_2/ha/h)/($J/m^2/s$)
E_a	Actual soil evaporation (cm)
E_{EQ}	Equilibrium evapotranspiration (cm)
Eh, ΔEh	Redox potential and its daily increase (mV)
E_p	Potential evaporation (cm)
ET_p	Potential evapotranspiration (cm)
f_{Clay}	Effects of clay adsorption on nitrogen gas emissions
f_{CO2}	Effects of CO_2 concentration on photosynthesis
$f_{D,E}$	Effects of soil moisture on soil evaporation
f_{DL}	Crop photoperiodism parameter for the sensitivity to day length
f_{Eh}	Effects of redox potential on methane production

$f_{NH4,l}$, $f_{NO3,l}$ Effects of ammonium and nitrate concentration on nitrogen uptake, respectively
f_{pHM} Effects of pH on methane production
$f_{pH,N}$ Effects of soil pH on nitrification
$f_{ROOT,l}$ Distribution factor for new root growth in soil profile
$f_s(T)$ Snow effects on canopy temperature
f_{TM} Effects of temperature on methane production
f_{TN} Effects of temperature on nitrification
f_{TP} Effects of temperature on photosynthesis rate at light saturation
$f_{W1,l}$, $f_{W2,l}$ Effects of moisture on water and nitrogen uptake, respectively
$F_{W,N}$ Effects of soil moisture on nitrification
F Fraction of assimilate partitioned to above ground organs
FC_l Soil moisture of layer l at field capacity (cm^3 water/cm^3 soil)
F_{DF} Fraction of diffuse light
$F_{N2O,\ NO}$, F_{N2} Fraction of N_2O, NO and N_2 emitted to the atmosphere, respectively
F_{NH4} Fraction of adsorbed NH_4^+
F_{RSl} Fraction of root senescence in layer l
F_{ROOTl} Fraction of the total root system (biomass or length) in layer l
F_{SL} Fraction of sunlit leaf area
GroL Daily growth of LAI (m^2 leaf/m^2 land)
G_s Concentration gradient of a solute (kg/ha cm water cm soil)
H_l, H_{l+1} Thickness of soil layer l and $l+1$ (cm)
I_0 Photosynthetically active radiation at a certain time of day(J/m^2/s)
I_{DF} Diffuse light because of atmosphere scattering (J/m^2/s)
I_{DR0}, I_{DR} Direct light above the canopy and accepted by sunlit leaves, respectively (J/m^2/s)
I'_{DR} Direct light in canopy if the leaves are non scattered back bodies (J/m^2/s)
I_{PDR} Light which is perpendicular to leave surface (J/m^2/s)
I_{SH} Light received by shaded leaves (J/m^2/s)
l Soil layer sequence number from the surface
J_s Solute flux (kg/d)
J_w Water flux (cm water/d)
JD, JD_0 Current Julian date and Julian date when solar altitude is the highest
K Light extinction coefficient for diffusion light in canopy
K_{35} Nitrification rate at 35 °C (25 mg/kg soil/d)
$K_{C,1/2}$ Half-saturation value of soluble carbon (0.017 kg C/m^3)
K_{Ci} Specific decomposition rate of carbon pool i (d^{-1})
K_{BL} Extinction coefficients of canopy assuming leaves are back bodies
$K_{DF,}$ K_{DR} Extinction coefficient of diffuse light and direct light in canopy, respectively
$K_{H2O,}$ K_{NH4} Dissociation constant for H^+ :OH^- equilibrium and NH_4^+ :NH_3 equilibrium, respectively
$K_{NxOy,1/2}$ Half-saturation value of NxOy (0.083 kg N/m^3)
LAI, ΔLAI Leaf area index and its daily increase (m^2 leaf/m^2 land)
L_i Leaf area index above layer i (m^2 leaf/m^2 land)
LL_l Soil moisture of layer l at wilting point (cm^3 water/cm^3 soil)
M_c, M_{NxOy} Maintenance coefficient of carbon (kg C/kg C/h) and NxOy (kg N/kg N/h), respectively
n, nr Total soil layers and soil layers influencing evaporation, respectively

ns	Nitrogen stress factor (0–1. 1 for not limiting effects, and 0 for completely limited)
N	Total nitrogen of $NxOy$ in a soil layer (kg N/ha)
N_{dem}	Total crop nitrogen demand in a day (g/m^2)
$N_{dem,d}$, $N_{dem,g}$	Crop nitrogen demand because of deficiency and growth, respectively (g/m^2)
NH_{4m}	NH_3 concentration in liquid phase (mol/l)
NH_4, $NH_{4p,l}$	NH_4^+ in a soil layer in kg N/ha and in ppm, respectively
$NO_{3p,l}$	Nitrate concentration in soil layer l (ppm)
$NO_{3,N}$	NH_4^+ converted to NO_3^- (kg N/ha/d)
N_R, N_{R0}, N_{Rmin}	Current, critical and minimum nitrogen concentration in root, respectively (g/g)
N_S, N_{S0}, N_{Smin}	Current, critical and minimum nitrogen concentration in shoot, respectively (g/g)
Nup	Nitrogen uptake capacity (g/m^2)
$NxOy$	Concentrations of NO_3^-, NO_2^- or N_2O in soil water (kg N/ha)
P_0	Daily gross photosynthesis (g/m^2)
P_i	Thermal time required for crop development in stage i (°C d)
$P(L_i,t_j)$	Photosynthesis at canopy layer L_i at time t_j (kg CO_2/ha/h)
pH	Soil pH
Phr	Phyllochron of wheat (95 °C d)
PI_{max}	Daily maximum plant interception (cm water)
P_{SH}, P_{SL}	Photosynthesis rate of shaded leaves and sunlit leaves, respectively (kg CO_2/ha/h)
Q_{10}	Crop maintenance respiration quotient (2.0)
R	Average specific root length (cm/g)
R_0	Root water uptake coefficient (0.003 cm water/cm root)
R_g, R_{g0}	Crop growth respiration (g/m^2) and average growth efficiency coefficient, respectively
Rld_l	Rood length density of layer l (cm root/cm^3 soil)
$R_{m,k}$, $R_{mo,k}$	Maintenance respiration (g/m^2) and maintenance respiration coefficient of crop organ k
$RT_{S,l}$, $RT_{A,l}$, $RT_{T,l}$, $RT_{N,l}$	Limiting factors for the effects of soil strength, aeration, temperature and nitrogen on rooting, respectively
Runoff	Daily surface runoff (cm)
s	Retention parameter for surface runoff estimation
S	Mid variable
$Sand_l$	Fraction of sand (2–0.05 mm) in layer l
S_c	Solute concentration in soil solution (kg/ha/cm water)
SC	Solar constant (J/m^2/s)
SD	Sowing depth (cm)
SenL	Daily LAI senescence rate (m^2 leaf/m^2 land)
Sh	Daily sunshine duration (hr)
Sla_0, Sla	Primary and current specific leaf area, respectively (m^2/g, $Sla_0 =$ 45 m^2/g)
SL_W, SL_N, SL_L, SL_T	Water, nitrogen, light (or density) and temperature effects stress on leaf senescence, respectively
Snow, SM_{max}	Snow and daily maximum snow melt (cm water)
SR_d	Daily solar radiation (J/m^2/s)
SW_l	Soil moisture of layer l (cm^3 water/cm^3 soil)
t, t_j	Time in a day (h)
T	Temperature for T_{max} and T_{min} (°C)
ΔT, ΔT_a	Daily range of extreme temperatures and its monthly average, respectively (°C)
T'	Temperature at sunset (°C)
T_{aa}, T_{am}	The amplitude and mean of annual temperature, respectively (°C)

$T_c(t)$	Canopy temperature at time t (°C)
T_{cd}, T_{cm}	Canopy daytime and daily mean temperature, respectively (°C)
$T_{c\ max}$, $T_{c\ min}$	Canopy daily maximum and minimum temperature, respectively (°C)
Tdtt	Thermal time accumulated in a stage (°C d)
T_{Db}, T_{Dm}	Base and maximum temperature of crop development (°C)
T_k, T_{k+1}	Soil surface temperature in day k and $k+1$
T_{max}, T_{min}	Daily air maximum and minimum temperature (input, °C)
T_s, T_{sl}	Soil daily temperature in current layer or layer l (°C)
T_p, T_a	Potential and actual crop transpiration (cm)
U_{DN}	Relative growth rate of denitrifiers
U_{NxOy}, $U_{NxOy,m}$	Relative growth rate and maximum growth rate of N_xO_y denitrifiers
UL_l	Soil porosity of layer l (cm^3 void/cm^3 soil)
v	Average pore water velocity ($=J_w/SW_l$ cm water/d)
W	Water input to soil surface (cm)
w_{1i}, w_{1j}	Gaussian integration weighting factors, 0.5–$0.15^{1/2}$, 0.5, 1–$0.15^{1/2}$ for w_{11}, w_{12} and w_{13}, respectively
w_{2i}, w_{2j}	Gaussian integration weighting factor, 1/3.6, 1.6/2.3 and 1/3.6 for w_{21}, w_{22} and w_{23}, respectively
$W_{fps,l}$	Soil moisture of a layer (fraction of water filled pore space)
ws	Water stress factor (0–1. 1 for not limiting effects, and 0 for completely limited)
Wup_l	Water uptake from layer l (cm)
x, x_1–x_4	Mid variables
Xs	A continuous phenological development scale
Y_c, Y_{NxOy}	Maximum growth yield on soluble carbon (kg C/kg C) and on N_xO_y (kg C/kg N), respectively
z_S	Zadokes development scale
Z_l, Z_{ne}	Depth of layer l, and depth of top soil affecting evaporation (20 cm), respectively (cm)
α, α_0	Albedo of the field and bare soil, respectively
α_h, α_s	Reflectivity of horizontally and spherically distributed canopy, respectively
β	The elevation angle of the sun (gradient)
π	3.14159
θ_l, θ_{l-1}	Soil moisture above wilting point of layer l and $l-1$ (cm^3 water/cm^3 soil)
φ	Latitude (gradient)
ω	Solar declination (gradient)
μ	Crop parameter for CO_2 effects on photosynthesis (0.4 and 0.8 for C4 and C3 plants, respectively)
μ_{clay}, μ_{CN}	Reduction factor of clay adsorption and C/N ratio on decomposition, respectively
$\mu_{pH,NxOy}$	Reduction factor of soil pH on denitrifier growth
μ_T, μ_{Til}, μ_W	Reduction factor of temperature, tilling and soil moisture on decomposition, respectively
$\mu_{T,DN}$	Reduction factor of temperature on denitrification
σ	Scatter coefficient (0.2)

References

Adams, R.M., Rosenzweig, C.R., Peart, R.M., Ritchie, J.T., McCarl, B.A., Glyer, J.D., Curry, R.B., Jones, J.W., Boote, K.J., Allen, L.H., Jr. 1990. Global climate change and US agriculture. Nature, 345, 219–224.

Albritton, D.L., Derwent, R.G., Isaksen, S.A., Lai, M., Wuebbles, D.J., 1995. Trace gas radiative forcing indices. In: Houghton, J.T., Meira Filho, L.G., Bruce, J., Lee, H., Callander, B.A., Haites, E., Harris, H., Maskell, K. (Eds.), Climate Change 1994: Radiactive Forcing of Climate Change. Cambridge University Press, Cambridge, England, pp. 11–16.

Biggar, J.W., Nielsen, D.R., 1976. Spatial variability of the leaching characteristics of a field soil. Water Resource. Res. 12, 78–84.

Briston, K.L., Cambell, G.S., 1984. On the relationship between incoming solar radiation and daily maximum and minimum temperature. Agric. For. Meteorol. 31, 159–166.

Cao, M., Dent, J.B., Heal, O.W., 1995. Modeling methane emissions from rice paddies. Global Biogeochem. Cycles 9, 193–195.

Chen, J.-L., Reynolds, J.F., 1997. GePSi: a generic plant simulator based on object-oriented principles. Ecol. Model. 94, 53–66.

Crill, P.P., Keller, M., Weitz, A., Grauel, B., Veldkamp, E., 2000. Intensive field measurements of nitrous oxide emissions from a tropical agricultural soil. Global Biogeochem. Cycles 14, 85–95.

Dickinson, R.E., Henderson-Sellers, A., Kennedy, P.J., Wilson, M.F., 1986. Bioshpere atmosphere transfer scheme (BATs) for NCAR community climate model. NCAR Tech. Note. TN275 + STR, pp. 69.

Dhakhwa, G.B., Campbell, C.L., LeDuc, S.K., Cooter, E.J., 1997. Maize growth: assessing the effects of global warming and CO_2 fertilization with crop models. Agric. For. Meteorol. 87, 253–272.

Duxbury, J.M., Harper, L.A., Mosier, A.R., 1993. Contributions of agroecosystems to global climate change. American Society of Agronomy, Crop Science Society of America, and Soil Science Society of America. Agricultural ecosystem effects on trace gases and global climate Change. ASA Special Publication No. 55, Madison, WI, pp. 1–18.

Gao, L., Jin, Z., Huan, Y., 1992. An Optimizing Decision Making System for Rice Culture. China Agricultural Science and Technology Press, Beijing.

Godwin, D.C., Jones, C.A., 1991. Nitrogen dynamics in soil plant system. In: Hanks, R.J., Ritchie, J.T. (Eds.), Modeling plant and soil system. Agronomy Monograph No. 31, pp. 287–322.

Goudriaan, J., 1986). A simple and fast numerical method for commutation of daily totals of crop photosynthesis. Agric. For. Meteorol. 38, 249–254.

Goudriaan, J., Laar, H.H., van Keulen, H., Louwerse, W., 1984. Simulation of the effect of increase atmospheric CO_2 on assimilation and transpiration of a closed crop canopy, Wissenschafliche Zeitchrift Humbolt Universitaet Berlin. Math.-Nat. R. 33 (4), 32–356.

Grant, R.F., 1998. Simulation in *ecosys* of root growth response to contrasting soil water and nitrogen. Ecol. Model. 107, 237–264.

Jenkinson, D.S., 1990. The turnover of organic carbon and nitrogen in soil. Philos. Trans. R. Soc. B 329, 361–368.

Jones, C.A., Kiniry, J.R., 1986. CERES—Maize: a simulation model of maize growth and development. Texas A&M University Press, College Station, TX, pp. 194.

Jones, C.A., Bland, W.L., Ritchie, J.T., Williams, J.R., 1991. Simulation of root growth. In: Hanks, J., Ritchie, J.T. (Eds.), Modeling Plant and Soil Systems. Agronomy Monograph No. 31, Madison, WI, pp. 91–123.

Kiniry, J.R., 1991. Maize phasic development. In: Hanks, R.J., Ritchie, J.T. (Eds.), Modeling Plant and Soil System. Agronomy Monograph No. 31, pp. 55–70.

Kropff, M.J., van Laar, H.H., 1993. ORYZA1—a basic model for irrigated low land rice production. IRRI, Philippines–Wageningen.

Li, C., 2000. Modeling trace gas emissions from agricultural ecosystems. Nutrient Cycling in Agroecosystems, 58 259–276.

Li, C., Frolking, S., Frolking, T.A., 1992a. A model of nitrous oxide evolution from soil driven by rainfall events: 1. Model structure and sensitivity. J. Geophys. Res. 97 (D9), 9759–9776.

Li, C., Frolking, S., Frolking, T.A., 1992b. A model of nitrous oxide evolution from soil driven by rainfall events: 2. Model application. J. Geophys. Res. 97 (D9), 9777–9783.

Li, C., Frolking, S., Harriss, R.C., Terry, R.E., 1994a. Modeling nitrous oxide emissions from agriculture: a Florida case study. Chemosphere 28, 1401–1415.

Li, C., Frolking, S., Harriss, R.H., 1994b. Modeling carbon biochemistry in agricultural soils. Global Bioheochem. Cycles 8, 237–254.

Li, C., Narayanan, V., Harriss, R.C., 1996. Model estimates of nitrous oxide emissions from agricultural lands in the United States. Global Biogeochem. Cycles 10, 297–306.

Li, C., Frolking, S., Crocker, G.J., Grace, P.R., Klir, J., Korchens, M., Poulton, P.R., 1997. Simulation trends in soil organic carbon in long-term experiments using the DNDC model. Geoderma 81, 45–60.

McCree, K.J., 1979. An equation for the rate of respiration of white clover plants grown under controlled conditions. In: Setlik, I. (Ed.), Prediction and Measurement of Photosynthetic Production. Pudoc, Wageningen.

Odell, R.T., Melsted, S.W., Walker, W.M., 1984. Changes in organic carbon and nitrogen of Morrow Plot soils under different treatments, 1904–1973. Soil Sci., 137, 161–171.

Parton, W.J., Stewart, J.W.B., Cole, C.V., 1988. Dynamics of C, N, P, and S in grass soils: a model. Biogeochemistry 5, 109–131.

Penning de Vries, F.W.T., Jansen, D.M., Ten Berge, H.F.M., Bakema, A., 1989. Simulation of Ecophysiological Processes of Growth in Several Annual Crops. Pudoc, Wageningen.

Potter, C.S., Matson, P.A., Vitousek, P.M., Davidson, E.A., 1996. Process modeling of controls on nitrogen trace gas emissions from soil world-wide. J. Geophys. Res. 101, 1361–1377.

Priestly, C.H.B., Taylor, R.J., 1972). On the assessment of surface heat flux and evaporation using large scale parameters. Monthly Weather Rev. 100, 81–92.

Project of Crop Water Stress and Drought in North China Plain, 1992. Crop Water Stress and Drought. Henan Science and Technology Press, Zhenzhao, China, pp. 289.

Ritchie, J.T., 1972. Model for predicting evaporation from a row crop with incomplete cover. Water Resources Res. 8, 1204–1213.

Ritchie, J.T., 1991. Wheat phasic development. In: Hanks, R.J., Ritchie, J.T. (Eds.), Modeling Plant and Soil System. Agronomy Monograph No. 31, pp. 31–54.

Ritchie, J.T., Godwin, D.C., Otter-Nache, S., 1988. CERES—Wheat. A simulation model of wheat growth and development. Texas A&M University Press, College Station, TX.

Ritchie, J.T., Alocilja, E.C., Singh, U., Uehara, G., 1987. IBSNAT and CERES—Rice model. Weather and Rice, Proceedings of the International Workshop on the Impact of Weather Parameters on Growth and Yield of Rice, 7–10 April 1986. International Rice Research Institute, Manilla, Philippines, pp. 271–281.

Sass, R.L., Fisher, F.M., Harcombe, P.A., Turner, F.T., 1990. Methane production and emission in a Texas rice field. Global Biogeochem. Cycles 4, 47–68.

Sass, R.L., Fisher, F.M., Harcombe, P.A., Turner, F.T., 1991a. Mitigation of methane emissions from rice fields: possible adverse effects of incorporated rice straw. Global Biogeochem. Cycles 5, 275–287.

Sass, R.L., Fisher, F.M., Turner, F.T., Jund, M.F., 1991b. Methane emission from rice fields as influenced by solar radiation, temperature, and straw incorporation. Global Biogeochem. Cycles 5, 335–350.

Sass, R.L., Fisher, F.M., Wang, Y.B., Turner, F.T., Jund, M.F., 1992. Methane emission from rice field: the effect of floodwater management. Global Biogeochem. Cycles 6, 249–262.

Sass, R.L., Fisher, F.M., Lewis, S.T., Turner, F.T., Jund, M.F., 1994. Methane emission from rice field: effect of soil properties. Global Biogeochem. Cycles 8, 135–140.

Saxton, K.E., Rawls, W.J., Romberger, J.S., Papendick, R.J., 1986. Estimating generalized soil–water characteristics from texture. Soil Sci. Soc. Am. J. 50, 1031–1036.

Sellers, P.J., Mintz, Y., Sud, Y.C., Dalcher, A., 1986. A simple biosphere model (SiB) for use within general circulation models. J. Atmos. Sci. 43 (6), 505–531.

Sigren, L.K., Byrd, G.T., Fisher, F.M., Sass, R.L., 1997a. Comparison of soil acetate concentrations and methane production, transport, and emission in two rice cultivars. Global Biogeochem. Cycles 11, 1–14.

Sigren, L.K., Lewis, S.T., Fisher, F.M., Sass, R.L., 1997b. Effects of field drainage on soil parameters related to methane production and emission from rice paddies. Global Biogeochem. Cycles 11, 151–162.

Spitters, C.J.T., Toussaint, H.A.J.M., Goudriaan, J., 1986. Separating the diffuse and direct component of global radiation and its implications for modeling canopy photosynthesis. Part I: components of incoming radiation. Agric. For. Meteorol. 38, 217–229.

Spitters, C.J.T., 1986. Separating the diffuse and direct component of global radiation and its implications for modeling canopy photosynthesis. Part II: calculation of canopy photosynthesis. Agric. For. Meteorol. 38, 231–242.

Tsuji, G.Y, Uehara, G., Balas, S. (Eds.), 1994. DSSAT v3. University of Hawaii, Honolulu, Hawaii.

US Department of Agriculture (USDA), Soil Conservation Service (SCS), 1972. Engineering field manual for conservation practice. USDA Soil Conservation Service, Washington, DC.

Vitousek, P.M., Aber, J.D., Howarth, R.W., Likens, G.E., Matson, P.A., Schindler, D.W., Schlesinger, W.H., Tilman, D.G., 1997. Human alteration of the global nitrogen cycle: sources and consequences. Ecol. Appl. 7, 735–750.

William, J.P., Logan, J.A., 1981. A model for diurnal variation in soil and air temperature. Agric. Meteorol. 23, 205–216.

Williams, J.R., 1995. The EPIC model. In: Singh, V.P. (Ed.), Computer Models of Watershed Hydrology. Water Resources Publications, Highlands Ranch, CO, pp. 909–1000.

de Wit, C.T., 1978. Simulation of assimilation, respiration and transpiration of crops. In: Simulation Monographs, vol. 2. Pudoc, Wageningen.

Yoshida, S., 1972. Physiological aspects of grain yield. Annu. Rev. Plant Physiol. 23, 437–464.

Zhang, Y., 1999. PhD thesis. Peking University, Beijing, China.